PLOS ONE

RESEARCH ARTICLE

A new 10-D hyperchaotic system with coexisting attractors and high fractal dimension: Its dynamical analysis, synchronization and circuit design

Khaled Benkouider[1], Toufik Bouden[1], Aceng Sambas[2], Badis Lekouaghet[1], Mohamad Afendee Mohamed[3]*, Sulaiman Ibrahim Mohammed[4,5], Mustafa Mamat[3], Mohd Asrul Hery Ibrahim[6], Muhammad Zaini Ahmad[7]

1 Automatic Department, University of MSB Jijel, Ouled Aissa, Jijel, Algeria, **2** Department of Mechanical Engineering, Universitas Muhammadiyah Tasikmalaya, Tasikmalaya, West Java, Indonesia, **3** Faculty of Informatics and Computing, Universiti Sultan Zainal Abidin, Kuala Terengganu, Malaysia, **4** School of Quantitative Sciences, College of Art and Sciences, Universiti Utara Malaysia, Sintok, Kedah, Malaysia, **5** Institute of Strategic Industrial Decision Modelling (ISIDM), School of Quantitative Sciences, Universiti Utara Malaysia, UUM Sintok, Kedah, Malaysia, **6** Faculty of Entrepreneurship and Business, Universiti Malaysia Kelantan (UMK), Kota Bharu, Kelantan, Malaysia, **7** Institute of Engineering Mathematics, Universiti Malaysia Perlis, Kuala Perlis, Arau, Perlis, Malaysia

* mafendi@unisza.edu.my

Citation: Benkouider K, Bouden T, Sambas A, Lekouaghet B, Mohamed MA, Ibrahim Mohammed S, et al. (2022) A new 10-D hyperchaotic system with coexisting attractors and high fractal dimension: Its dynamical analysis, synchronization and circuit design. PLoS ONE 17(4): e0266053. https://doi.org/10.1371/journal.pone.0266053

Editor: Esteban Tlelo-Cuautle, Instituto Nacional de Astrofisica Optica y Electronica, MEXICO

Received: November 15, 2021

Accepted: March 11, 2022

Published: April 12, 2022

Data Availability Statement: All relevant data are within the manuscript.

Funding: This work was supported by Universiti Sultan Zainal Abidin, Terengganu, Malaysia, 450 under the Center of Research Excellence & Incubation Management. The funders had no role in study design, data collection and analysis, decision to publish, or preparation of the manuscript.

Abstract

This work introduce a new high dimensional 10-D hyperchaotic system with high complexity and many of coexisting attractors. With the adjustment of its parameters and initial points, the novel system can generate periodic, quasi-periodic, chaotic, and hyperchaotic behaviours. For special values of parameters, we show that the proposed 10-D system has a very high Kaplan-Yorke fractal dimension, which can reach up to 9.067 indicating the very complexity of the 10-D system dynamics. In addition, the proposed system is shown to exhibit at least six varied attractors for the same values of parameters due to its multistability. Regions of multistability are identified by analysing the bifurcation diagrams of the proposed model versus its parameters and for six different values of initial points. Many of numerical plots are given to show the appearance of different dynamical behaviours and the existence of multiple coexisting attractors. The main problem with controlling chaos/hyperchaos systems is that they are not always fully synchronized. therefore, some powerful synchronization techniques should be considered. The synchronization between the high-dimensional 10-D system and a set of three low-dimensional chaotic and hyperchaotic systems is proposed. Ten control functions are designed using the active control method, ensuring synchronisation between the collection of systems and the 10-D hyperchaotic system. Finally, using Multisim 13.0 software to construct the new system's electronic circuit, the feasibility of the new system with its extremely complicated dynamics is verified. Therefore, the novel 10-D hyperchaotic system can be applied to different chaotic-based application due to its large dimension, complex dynamics, and simple circuit architecture.

Competing interests: The authors have declared that no competing interests exist.

Introduction

Scientific communities have been interested in chaotic systems study over the past 60 years, especially since the work of Edward Lorenz, the famous American meteorologist in 1963 [1]. The essential trait of chaotic systems, he discovered, is their great sensitivity to initial conditions. A small change in the chaotic system's initial parameters results in significantly varied and unpredictable behaviour. This type of system's tremendous complexity makes it beneficial in a variety of fields, including secure communication [2–5].

The Kaplan-Yorke dimension and the Lyapunov exponents are the most important tools for describing chaotic behaviour in a dynamical system [6]. Kaplan-Yorke dimension, on the other hand, is an effective measure of the fractal dimension and chaotic complexity of the normal n-dimensional dynamical system, and it is calculated using Lyapunov exponent values. When calculating the Lyapunov exponent, the dynamical system's two adjacent starting values are taken into account. The paths produced via the initial guesses will exponentially diverge if this system exhibits chaotic behaviour, and the coefficients that characterises the divergence rate is a Lyapunov exponent. There is, absolutely, a Lyapunov exponent for every state-space dimension. At least one of the exponents must be positive for a dynamic system to display chaotic behavior. When there are many non-negative exponents, the related systems' dynamics expand in multiple directions, resulting in a more complex behaviour, which we name a hyperchaotic system in this situation.

Many papers have been published on hyperchaotic system. Vaidyanathan et al. [7] proposed of the new 4-D hyperchaotic system with no equilibrium and analysis of global hyperchaos synchronization results of the new hyperchaotic system using Integral Sliding Mode Control (ISMC). Singh et al. [8] proposed of the 5-D hyperchaotic system with stable equilibrium point and the proposed system exhibits multistability and transient chaotic behavior. Alattas et al. [9] proposed of the synchronization problem of hyperchaotic systems using integral-type sliding mode control for the 6-D hyperchaotic systems and presented of the analog electronic circuit using MultiSIM. Lagmiri et al. [10] constructed of the two new 7D hyperchaotic systems and to investigate the dynamics and synchronization of these new systems using the theory of observers. Kang et al. [11] proposed a color image encryption method combining with 2D-VMD and 8D hyperchaotic system. Zhu et al [12] presented a nine-dimensional eight-order chaotic system, and the corresponding circuit implementation. Mahmoud et al. [13] presented another complex nonlinear hyperchaotic model, spoke to by nine first-order nonlinear ordinary differential equations and proposed new nine-dimensional chaotic Lorenz System with quaternion variables [14]. Jianliang et al. [15] proposed a ten-dimensional nine-order chaotic system and the electronic circuit implementation. However, there is still a need for discovering systems with different 10D hyperchaotic system.

Synchronization of chaotic systems has attracted much attention in recent years due to their applications in neuron model, robotic and cryprosystem. Yu et al. [16] presented a novel 5D hyperchaotic four-wing memristive system with multiline equilibrium and synchronization of the 5D hyperchaotic system with different structures by active control. Zambrano-Serrano and Anzo-Hernández [17] proposed a novel chaotic oscillator derived from the generic four-dimensional autonomous jerk systems and analyze the synchronization behavior of the chaotic oscillator via feedback control. Munoz-Pacheco et al. [18] analyzed the effect of a non-local fractional operator in an asymmetrical glucose-insulin regulatory system and proposed an active control scheme for forcing the chaotic regime (an illness) to follow a periodic oscillatory state, i.e., a disorder-free equilibrium. However, to the best of the authors' knowledge, neither the control nor the synchronisation of the new 10-D hyperchaotic system has been investigated yet with the active control method.

Secure transmissions utilising various methods and schemes is one of chaotic system's most essential applications. Chaotic systems generate complex signals with a random appearance, which are used to conceal the secret information to be communicated. As a result, many literature have studied the chaotic systems, so as to address the huge gap for the type of complicated system in the disciplines of chaotic encryption and secure communication [19, 20]. Nazari et al. [21] proposed secure transmission of authenticated medical images using a novel chaotic IWT-LSB blind watermarking approach. design an embedded cryptosystem based on a pseudo-random number generator (PRNG). Trujillo-Toledo et al. [22] proposed design an embedded cryptosystem based on a pseudo-random number generator (PRNG)using enhanced sequences from the Logistic 1D map, and it reaches a throughput of up to 47.44 Mbit/s using a personal computer with a 2.9 GHz clock, and 10.53 Mbit/s using a Raspberry Pi 4. Hemdan [23] presented a medical image watermarking approach based on Wavelet Fusion (WF), Singular Value Decomposition (SVD), and Multi-Level Discrete Wavelet Transform (M-DWT) with scrambling techniques for securing the watermarks images. García-Guerrero et al. [24] introduces a process to improve the randomness of five chaotic maps that are implemented on a PIC-microcontroller. They have improved chaotic maps tested to encrypt digital images in a wireless communication scheme, particularly on a machine-to-machine (M2M) link, via ZigBee channels. Silva-Juárez et al. [25] proposed the use of first-order all-pass and low-pass filters to design the ratio of the polynomials that approximate the fractional-order. Also, the filters are implemented using amplifiers and synthesized on a field-programmable analog array (FPAA) device. Tlelo-Cuautle et al. [26] provides guidelines to implement fractional-order derivatives using commercially available devices and describes details on using FPGAs to approach fractional-order chaotic systems, programming in VHDL and reducing hardware resources.

In addition, as previously stated, several studies discovered that the hyperchaotic systems with high dimensional ($n > 3$) whose positive Lyapunov exponent is more than one and having a high Kaplan-Yorke dimension is capable of generating more random and complex signals with greater uncertainty, which improves the chaotic transmissions security. Based of these reasons, several types of these high dimensional systems have been developed having two positive Lyapunov exponents since after the emergence the first system by Rossler in 1979 [27]. Some nonlinear dynamical systems can develop many forms of complexity such as chaos, hyperchaos, bifurcation and multistability. A dynamical system that generate two or more synchronize different attractors for a given set of coefficients is defined to be multistable.

In the recent years, construction new high dimensional ($n > 5$) hyperchaotic systems with high fractal dimension [28] and extreme multistability become an interesting area of research in chaos theory because of the need of these kinds of hyper-complex systems in recent engineering applications especially in secure communications. In this work, we generate the first 10-D hyperchaotic system which exhibit up to six synchronize attractors having high Kaplan-Yorke fractal dimension. The new 10-D hyperchaos system's dynamic properties is discussed, its Regions of multistability identified, its active control synchronization and design its equivalent electronic circuit described.

The novelty and contributions of the paper are summarised as follows:

1. System has four positive parameters, twenty-three terms with two quadratic and one quartic nonlinearity.
2. This work reports various types of complexity behaviors in 10D hyperchaotic system, such as Chaos, Hyperchaos and Quasi-Periodic.
3. System has multistability, i.e. coexistence of chaotic attractors under various conditions.

4. System has unstable and self-excited family.
5. This work studied the synchronization of the proposed 10D system with three diverse Hyperchaotic and chaotic systems via active controllers.
6. The equivalent electronic circuit for the new 10-D hyperchaotic system (1) is developed using Multisim 13.0 software.

The rest of this paper is organized as follows. Section 2 describes the dynamics of the new 10D Hyperchaotic system. Dynamical analyses of the new 10D Hyperchaotic system are shown in Section 3. multistability and coexisting attractors in the new 10D Hyperchaotic system is discussed in Section 4. In Section 5 we discuss the synchronization of the new 10D hyperchaotic systems using active control. Circuit implementation of the new 10-D hyperchaotic system are presented in Section 6. Finally, the conclusions of this paper are summarized in Section 7.

New 10-D hyperchaotic system

There are four positive parameters in the new 10D hyperchaotic system, as well as twenty-three terms with two quadratic and one quartic nonlinearity. The new system is describe using the algebraic equations (1):

$$\begin{cases} \dot{x_1} = x_3 + x_1x_2 - x_1, \\ \dot{x_2} = 1 + a(x_2 - x_1^4) - x_1^2, \\ \dot{x_3} = -x_1 + x_3 + x_4, \\ \dot{x_4} = -bx_3 + cx_5, \\ \dot{x_5} = -x_4 + x_6, \\ \dot{x_6} = -x_5 + x_7, \\ \dot{x_7} = -x_6 + x_8, \\ \dot{x_8} = -x_7 + (1-d)x_9, \\ \dot{x_9} = -x_8 + x_{10}, \\ \dot{x_{10}} = -x_9 + x_7. \end{cases} \tag{1}$$

where the state variables are given as x_1, x_2, x_3, x_4, x_5, x_6, x_7, x_8, x_9 and x_{10} while a, b, c and d parameters denote the positive constant. When the initial guess are selected as:

$$(1, 0, 0, 0, 0, 0, 0, 0, 0, 0). \tag{2}$$

and the coefficient values are selected as:

$$a = 0.1,\ \ b = 0.1,\ \ c = 1.1,\ \ d = 0.01. \tag{3}$$

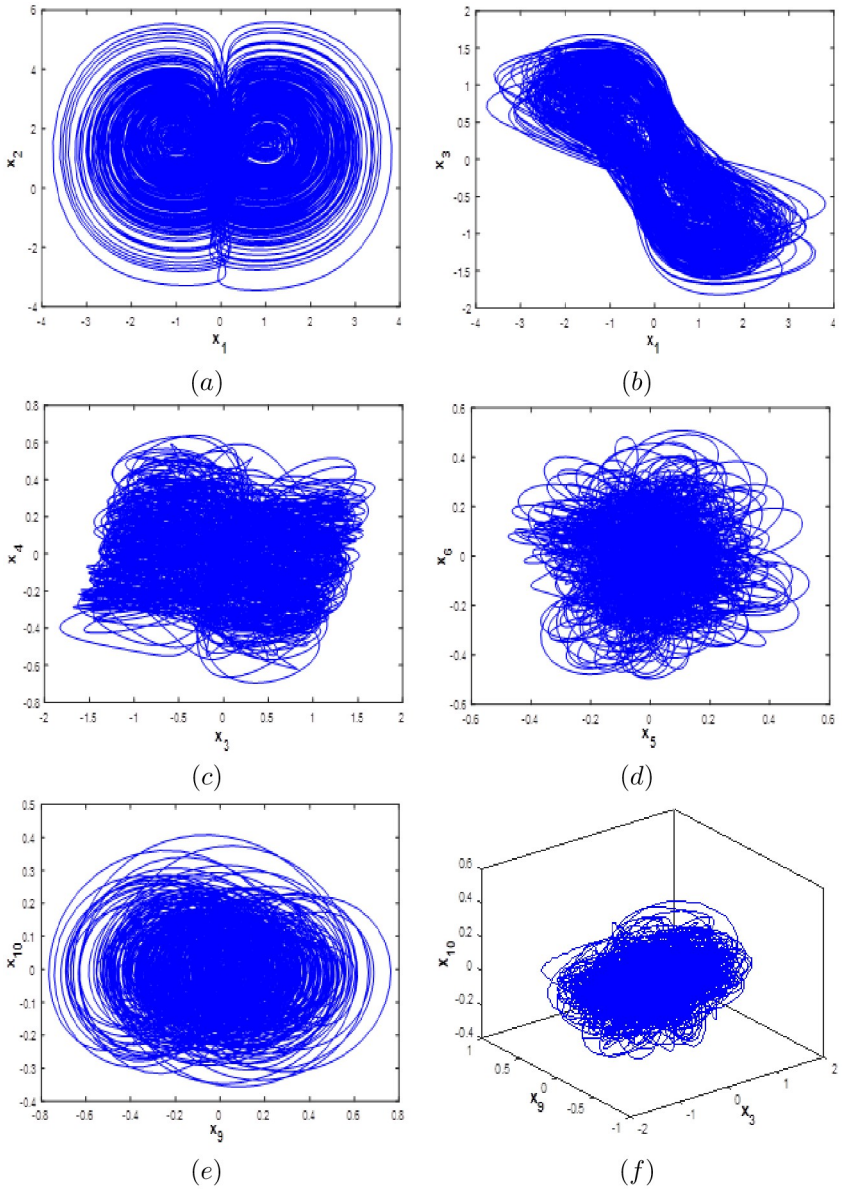

Fig 1. Phase portraits of the 10-D hyperchaotic system (1): (a) $x_1 - x_2$ attractor, (b) $x_1 - x_3$ attractor, (c) $x_3 - x_4$, (d) $x_5 - x_6$ attractor, (e) $x_9 - x_{10}$ attractor and (f) $x_3 - x_9 - x_{10}$ attractor.

https://doi.org/10.1371/journal.pone.0266053.g001

System (1) exhibit a complex hyperchaotic behavior with high fractal dimension and its phase portraits are described in Fig 1 using the Matlab ode45 function. It clear from the Fig 1 that our proposed the new 10D hyperchaotic system generates two-wing attractors.

The Lyapunov exponents (*LE*) for the new 10D hyperchaotic system (1) whose initial conditions is given in Eq (2) and the parameters values as in Eq (3) can be calculated using Wolf's algorithm, results are shown in Fig 2.

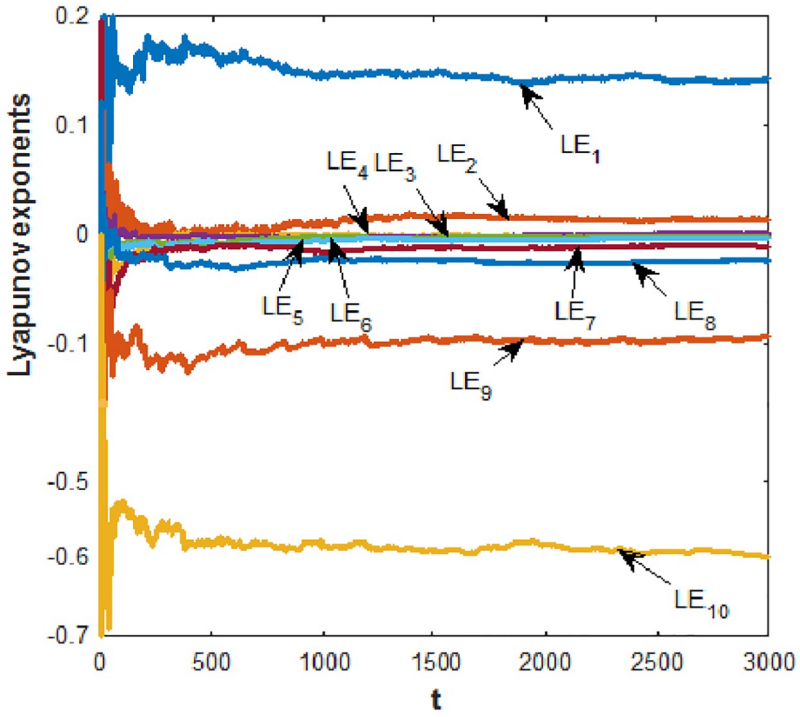

Fig 2. Lyapunov exponents of the new 10-D hyperchaotic system (1) with a = 0.1, b = 0.1, c = 1.1 and d = 0.01.

https://doi.org/10.1371/journal.pone.0266053.g002

The obtained ten *LE* of the new 10D hyperchaotic system (1) are:

$$\begin{cases} LE_1 = 0.142, \\ LE_2 = 0.038, \\ LE_3 = 0, \\ LE_4 = 0, \\ LE_5 = 0, \\ LE_6 = 0, \\ LE_7 = -0.011, \\ LE_8 = -0.024, \\ LE_9 = -0.094, \\ LE_{10} = -0.597. \end{cases} \tag{4}$$

As shown in Fig 2, system (1) has $LE_{1,2} > 0$, $LE_{3,4,5,6} = 0$, $LE_{7,8,9,10} < 0$, which means that it exhibits a hyperchaotic behavior with two positive, four zero and four negative *LE*. The sum of the *LE* is also negative, indicating that our suggested 10-D system (1) is dispersed.

According to chaos theory, Kaplan-Yorke dimensions high value directly corresponds to system dynamics' high complexity. For the proposed system (1), the analogous Kaplan-Yorke

dimension is calculated as follows:

$$D_{KY} = j + \frac{1}{\mid L_{j+1} \mid} \sum_{j=1}^{j} L_j. \tag{5}$$

with j representing the index such that:

$$\sum_{i=1}^{j} L_j > 0 \ \ and \ \sum_{i=1}^{j+1} L_j < 0. \tag{6}$$

So, for (1), we discover that:

$$D_{KY} = 9 + \frac{\sum_{i+1}^{9} LE_i}{\mid LE_{10} \mid} = 9.045. \tag{7}$$

We can observe from (7) that fractal dimension of Kaplan-Yorke is very large in comparison to other systems. Thus, the proposed 10-D system (1) displays a very complex hyperchaotic behaviour.

Table 1 illustrate our new system (1) Kaplan-Yorke fractal dimension and that of some famous high dimensional recently reported hyperchaotic systems.

In 2011, J. C. Sprott [29] proposed three criteria for the publication of a new hyperchaotic system. It is said in [29], that a new system must satisfy at least one criterion. Among the three criteria, one criterion is that the system should exhibit some behavior previously unobserved. The new behavior of the new 10D hyperchaotic is compared in Table 1.

It can be seen from Table 1 that the 10-D system (1) has a more advanced fractal dimension than some famous high dimensional chaotic systems reported in literature, which indicate and prove the high complexity of system (1).

Dynamical analysis of the new 10-D hyperchaotic system

In this part, the effect of initial conditions and coefficient on the complexity and properties of system (1) would be studied. Stability of equilibrium points, Lyapunov exponents, fractal dimension and coexisting attractors will be the main properties of investigation.

Table 1. Kaplan-Yorke fractal dimension of ten high dimensional chaotic system.

System	Fractal dimension
7-D Varan system [30]	2.175
7-D Lagmiri system [10]	2.091
7-D Yu system [31]	5.278
7-D Yang system [32]	6.149
7-D Hu and Chan system [33]	6.732
9-D Zhu system [12]	2.171
9-D Mahmoud system [13]	5.065
9-D Mahmoud system [14]	5.128
10-D Jianliang system [15]	2.429
The new 10-D system (1)	9.045

https://doi.org/10.1371/journal.pone.0266053.t001

Equilibrium points and stability

The first step in dynamic analysis is solving the algebraic equations below to discover new 10-D hyperchaotic system (1) points of equilibrium:

$$\begin{cases} x_3 + x_1x_2 - x_1 = 0, \\ 1 + a(x_2 - x_1^4) - x_1^2 = 0, \\ -x_1 + x_3 + x_4 = 0, \\ -bx_3 + cx_5 = 0, \\ -x_4 + x_6 = 0, \\ -x_5 + x_7 = 0, \\ -x_6 + x_8 = 0, \\ -x_7 + (1-d)x_9 = 0, \\ -x_8 + x_{10} = 0, \\ -x_9 + x_7 = 0. \end{cases} \tag{8}$$

By considering the parameters values (3), three equilibrium points is obtained as the following:

$$\begin{cases} E_1 = [0, -10, 0, 0, 0, 0, 0, 0, 0, 0] \\ E_2 = [-1, 1, 0, -1, 0, -1, 0, -1, 0, -1] \\ E_3 = [1, 1, 0, 1, 0, 1, 0, 1, 0, 1] \end{cases} \tag{9}$$

We study the stability of (1) at the three equilibrium points by studying the eigenvalues of the following Jacobean of the 10-D system.

$$J_{E_i} = \begin{bmatrix} x_2 - 1 & x_1 & 1 & 0 & 0 & 0 & 0 & 0 & 0 & 0 \\ -2x_1 - 4ax_1^3 & a & 0 & 0 & 0 & 0 & 0 & 0 & 0 & 0 \\ -1 & 0 & 1 & 1 & 0 & 0 & 0 & 0 & 0 & 0 \\ 0 & 0 & -b & 0 & c & 0 & 0 & 0 & 0 & 0 \\ 0 & 0 & 0 & -1 & 0 & 1 & 0 & 0 & 0 & 0 \\ 0 & 0 & 0 & 0 & -1 & 0 & 1 & 0 & 0 & 0 \\ 0 & 0 & 0 & 0 & 0 & -1 & 0 & 1 & 0 & 0 \\ 0 & 0 & 0 & 0 & 0 & 0 & 1 & 0 & 1-d & 0 \\ 0 & 0 & 0 & 0 & 0 & 0 & 0 & -1 & 0 & 1 \\ 0 & 0 & 0 & 0 & 0 & 0 & 1 & 0 & -1 & 0 \end{bmatrix} \tag{10}$$

By considering the parameters values (3) the characteristic polynomial of J_{E_i} is calculated as:

$$\nabla(\lambda) = \lambda^{10} + 9.9\lambda^{9} - 4.81\lambda^{8} + 62.381\lambda^{7} - 57.222\lambda^{6} + 104.3812\lambda^{5} - 101.0089\lambda^{4} + 36.6971\lambda^{3} - 24.8579\lambda^{2} + 2.2209\lambda - 0.0011. \tag{11}$$

Then, the eigenvalues of J_{E_1} are obtained as:

$$\lambda_1 = -10.3161, \lambda_{2,3} = \pm 1.9358i, \lambda_4 = 0.2538, \lambda_{5,6} = 0.0058 \pm 1.4453i, \lambda_{7,8} = 0.0245 \pm 0.5498i, \lambda_9 = 0, \lambda_{10} = 0.1. \tag{12}$$

The characteristic polynomial of J_{E_2} is calculated as:

$$\nabla(\lambda) = \lambda^{10} - 1.1\lambda^{9} + 9.69\lambda^{8} - 9.209\lambda^{7} + 31.433\lambda^{6} - 25.5918\lambda^{5} + 36.7331\lambda^{4} - 25.9284\lambda^{3} + 8.9336\lambda^{2} - 5.5251\lambda + 0.0024. \tag{13}$$

Then, the eigenvalues of J_{E_2} are obtained as:

$$\lambda_{1,2} = 0.169 \pm 1.8045i, \lambda_{3,4} = 0.0021 \pm 1.9349i, \lambda_{5,6} = 0.0015 \pm 1.4339i, \lambda_7 = 0.7185, \lambda_{8,9} = 0.0179 \pm 0.549i, \lambda_{10} = 0. \tag{14}$$

The characteristic polynomial of J_{E_3} is calculated as:

$$\nabla(\lambda) = \lambda^{10} + 9.9\lambda^{9} - 4.81\lambda^{8} + 62.381\lambda^{7} - 57.22\lambda^{6} + 104.3812\lambda^{5} - 101.0089\lambda^{4} + 36.697\lambda^{3} - 24.8579\lambda^{2} + 2.2209\lambda - 0.0011. \tag{15}$$

Then, the eigenvalues of J_{E_3} are obtained as:

$$\lambda_1 = -10.9161, \lambda_2, 3 = \pm 1.9358i, \lambda_4 = 0.8538, \lambda_5, 6 = 0.0058 \pm 1.4453i, \lambda_7, 8 = 0.0245 \pm 0.5498i, \lambda_9 = 0, \lambda_1 0 = 0.1. \tag{16}$$

We observe the existence of four eigenvalues with positive real part in (12), nine positive eigenvalues in (14) and nine positive eigenvalues in (16) which shows that all equilibrium points are unstable. In addition, we can conclude that the 10-D system hyperchaotic attractor belongs to the self-excited family (1).

Bifurcation, Lyapunov exponents and fractal dimension

The *LE* spectrum and bifurcation diagram are two most significant tools for analyzing a system's dynamical behavior. The Kaplan-Yorke fractal dimension is also a useful indicator of system complexity. The dynamical behavior and complexity of the novel 10-D system (1) are examined using numerical simulations in this section of the study, with variable positive coefficient *a*, *b*, *c*, and *d*.

Parameter *a* varying. To investigate the sensitivity of (1) to the value of parameter *a*, we let $b = 0.1$, $c = 0.5$, $d = 0.01$ and vary *a* between 0 and 0.2. The bifurcation diagram (*BD*) of (1) with corresponding Lyapunov exponents spectrum when *a* belongs to the following set of values [0;0.2] and for initial conditions (3) are depicted in Fig 3, we can observe that *BD* and Lyapunov exponents spectrum are in good agreement. Fig 3 illustrate that the new 10-D system (1) can exhibit periodic behavior without positive Lyapunov exponents which means that the Kaplan-yorke fractal dimension equal to zero indicating no complexity of the dynamics. Also, the 10-D system can involves into a chaotic attractor or a hyperchaotic attractor with high Kaplan-Yorke fractal dimension which indicates complexity of the dynamics.

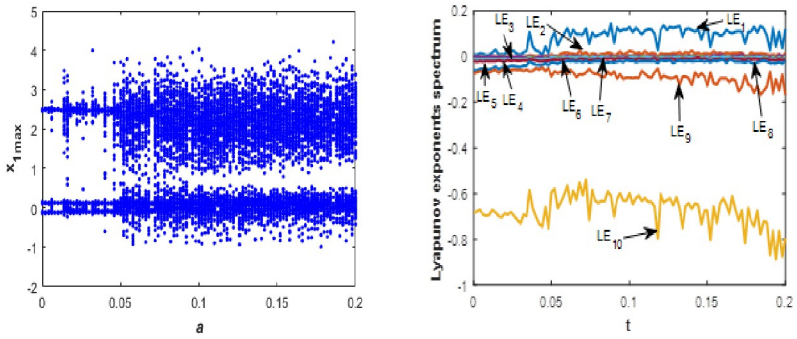

Fig 3. Bifurcation diagram (a) and Lyapunov exponents spectrum (b) of the new 10-D system (1) when: $b = 0.1$, $c = 1.8$, $d = 0.01$ and $a \in [0;0.2]$.

https://doi.org/10.1371/journal.pone.0266053.g003

When $a \in ([0, 0.013], [0.017, 0.021], [0.027, 0.031])$, the new 10-D system (1) exhibit a periodic behavior without complexity. When $a \in ([0.014, 0.016], [0.022, 0.026], [0.032, 0.042], [0.046, 0.050], [0.188, 2])$, the new 10-D system (1) generates a chaotic behaviour with different level of complexity. When a varies the value of kaplan-yorke dimension moves from 6.739 when $a = 0.035$ to 8.374 when $a = 0.195$. When $a \in ([0.050, 0.187])$, the new 10-D system (1) exhibits a hyperchaotic behavior with very high level of complexity. The corresponding kaplan-yorke dimension moves from a high value of 8.746 when $a = 0.185$ to a very high value of 9.067 when $a = 0.6$. Fig 4 illustrates several attractors and dynamical behaviors for various values of a. In addition, Table 2 shows the Kaplan-Yorke fractal dimension and Lyapunov exponents for some values of a.

Parameter *b* varying. To investigate the sensitivity of new 10-D hyperchaotic system (1) to the value of parameter b, we fix $a = 0.1$, $c = 1.8$, $d = 0.01$ and vary b between 0.1 and 2. Fig 5 gives the *LE* spectrum and *BD* of (1) when and for initial conditions (3), we can observe an excellent compatibility between *LE* spectrum and the corresponding *BD*.

It is obvious from Fig 5 that the proposed 10-D system (1) can exhibits periodic behaviour with Kaplan-yorke fractal dimension equal to zero indicating no complexity of the dynamics. Also, the 10-D system can involves into a chaotic attractor with one positive *LE* and a higher fractional Kaplan-Yorke dimension which indicates complexity of the dynamics. In addition, more complexity is observed when the new system generate a hyperchaotic behaviour with more than one positive *LE* and higher values of Kaplan-Yorke fractal dimension, which indicates a very complicated dynamic behavior generated by the new 10-D system (1).

When, the new 10-D system (1) associate into a hyperchaotic attractor with two positive *LE* and a very high complexity. The corresponding Kaplan-Yorke fractal dimension equal to: 6.597 when $b = 0.8$, 7.960 when $b = 0.42$, 8.165 when $b = 0.3$ and it can reach 9.064 when $b = 0.1$. These high values prove the very complex behavior of system (1). When, the new 10-D system (1) with one positive Lyapunov exponents generates a chaotic behavior, the corresponding Kaplan-Yorke fractal dimension equal to: 5.236 when $b = 0.95$ and 4.465 when $b = 1.16$. When, the new 10-D system (1) possesses a quasi-periodic behavior with two or three zero and eight negative *LE*s. Different dynamic behaviors and attractors for special values of the parameter$b$ are displayed in Fig 6. Table 3 shows the *LE* and the Kaplan-Yorke fractal dimension for different values of b.

Parameter *c* varying. To study 10-D system (1) sensitivity to the value of parameter c, we let $a = 0.1$, $b = 0.1$, $d = 0.01$ and vary c between 0 and 3. Fig 7 gives the *LE* spectrum and *BD* of

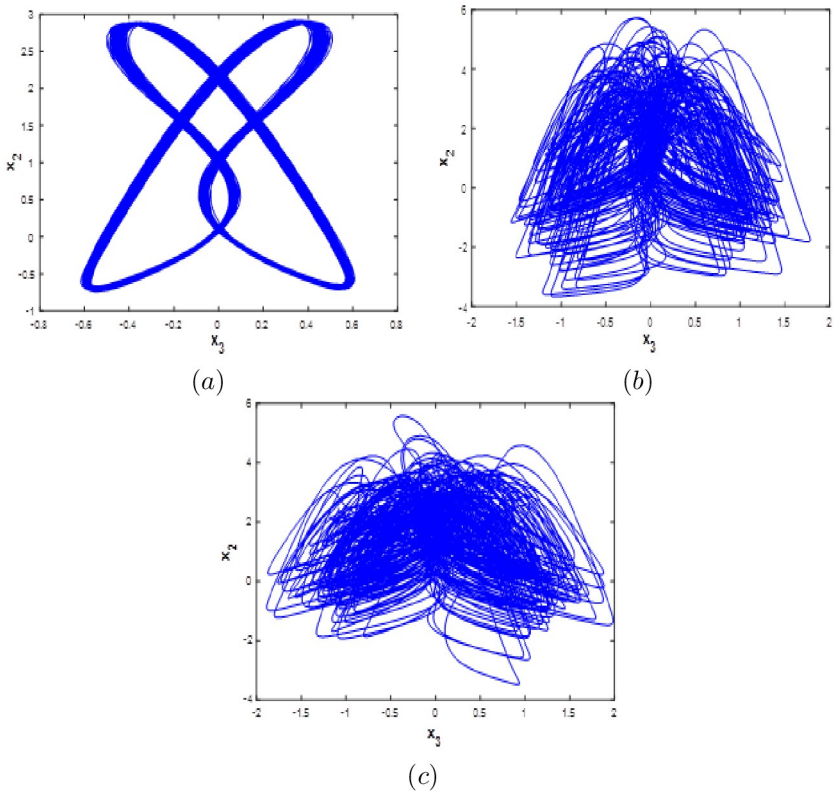

Fig 4. Phase portraits of the new 10-D system (1) for different values of *a*. (a) $x_3 - x_2$ Quasi-periodic attractor, (b) $x_3 - x_2$ chaotic attractor and (c) $x_3 - x_2$ hyperchaotic attractor.

https://doi.org/10.1371/journal.pone.0266053.g004

system (1) when and for initial conditions (3). From close observation of the figure, there is a good compatibility between Lyapunov exponents spectrum and the corresponding bifurcation diagram. When parameter c varies, we can see from Fig 7 that the new 10-D system (1) can exhibits periodic behavior with no complexity, chaotic behavior with one positive *LE* and a high fractional Kaplan-Yorke dimension, which illustrates complexity of the dynamics. In addition, higher complexity is observed when the proposed system generates a hyperchaotic behavior with more than one positive *LE* and higher values of fractional Kaplan-Yorke dimension. When c ([0, 0.05], [0.13, 0.15], [0.24, 0.26], [0.45, 0.70], [2.36, 3]) the new system (1) generates periodic behaviour where the corresponding Kaplan-Yorke fractal dimension equal to zero. When c ([0.06, 0.012], [0.17, 0.23], [0.27, 0.44], [0.71, 0.8], [1.92, 2.35], [2.65, 2.70], [2.85, 2.87]) the new 10-D system (1) involves into a chaotic attractor with different level of complexity. When $c = 0.1$, the value of Kaplan-Yorke fractal dimension is 6.676. This value may

Table 2. Lyapunov exponents, Kaplan-Yorke dimensin and dynamics of the new 10D system (1) with parameter *a* varying.

a	LE_1	LE_2	LE_3	LE_4	LE_5	LE_6	LE_7	LE_8	LE_9	LE_{10}	D_{KY}	Dynamics
0.06	0.132	0.015	0	0	0	0	-0.011	-0.018	-0.079	-0.578	9.067	Hyperhaos
0.185	0.111	0.014	0	0	0	0	-0.016	-0.015	-0.126	-0.723	8.746	Hyperhaos
0.195	0.134	0	0	0	0	-0.01	-0.012	-0.023	-0.238	-0.711	8.374	Chaos
0.035	0.027	0	0	0	0	-0.01	-0.023	-0.038	-0.056	-0.69	6.739	Chaos
0.01	0	0	0	0	-0.011	-0.012	-0.02	-0.056	-0.07	-0.693	0	Quasi-Periodic

https://doi.org/10.1371/journal.pone.0266053.t002

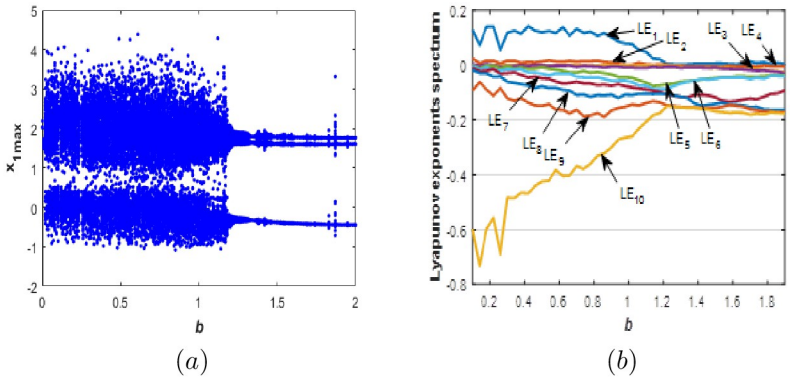

(a) (b)

Fig 5. Bifurcation diagram (a) and Lyapunov exponents spectrum (b) of the new 10-D system (1) when: $a = 0.1$, $c = 1.8$, $d = 0.01$ and $b \in [0.1;2]$.

https://doi.org/10.1371/journal.pone.0266053.g005

increase up to 7.163 when $c = 0.40$ providing a high complexity. When $c = 0.77$ we have obtained the highest value for chaotic attractors of system (1) which is 8.589. When, the new 10-D system (1) displays a hyperchaotic behavior with two positive, four zero and four negative *LE*. The corresponding Kaplan-Yorke fractal dimension is 9.031 when $c = 1.4$. Different attractors and dynamical behaviors for special values of the coefficient c are given in Fig 8. Table 4 shows the *LE* and fractional Kaplan-Yorke dimension for various values of c.

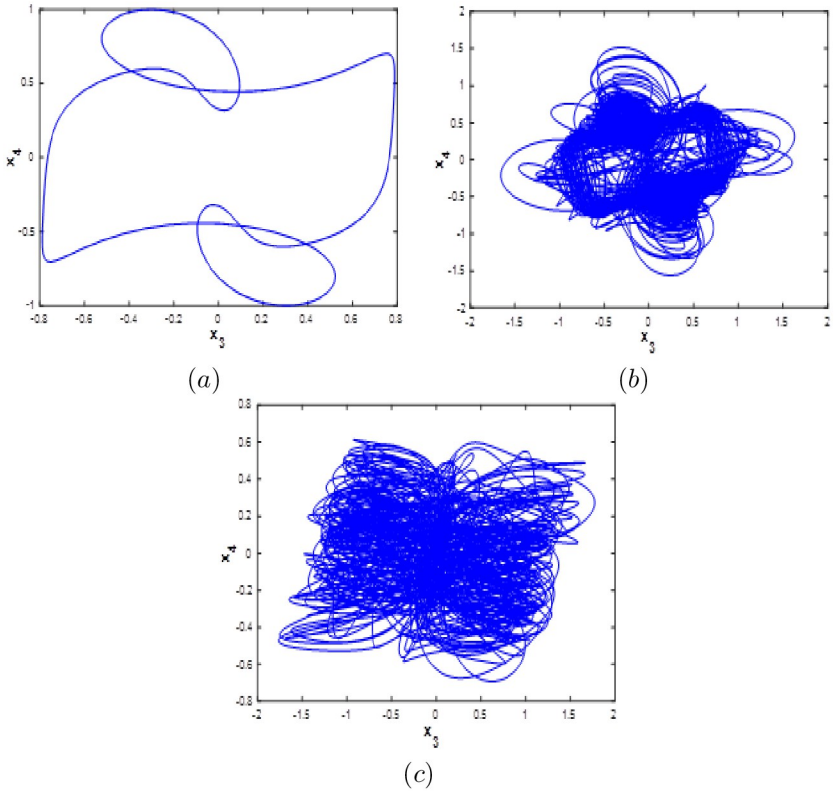

(a) (b) (c)

Fig 6. Phase portraits of the new 10-D system (1) for different values of *b*. (a)$x_3 - x_4$Periodic attractor, (b) $x_3 - x_4$ chaotic attractor and (c) $x_3 - x_4$ hyperchaotic attractor.

https://doi.org/10.1371/journal.pone.0266053.g006

Table 3. Lyapunov exponents, Kaplan-Yorke dimension and dynamics of the new 10D system (1) with parameter *b* varying.

b	LE_1	LE_2	LE_3	LE_4	LE_5	LE_6	LE_7	LE_8	LE_9	LE_{10}	D_{KY}	Dynamics
0.1	0.135	0.023	0	0	0	-0.01	-0.011	-0.014	-0.085	-0.593	9.064	Hyperchaos
0.3	0.12	0.014	0	0	-0.01	-0.013	-0.03	-0.061	-0.121	-0.497	8.165	Hyperchaos
0.42	0.129	0.016	0	0	-0.016	-0.022	-0.035	-0.075	-0.134	-0.468	7.96	Hyperchaos
0.8	0.118	0.013	0	-0.01	-0.029	-0.055	-0.062	-0.113	-0.176	-0.377	6.597	Hyperhaos
0.95	0.066	0	0	-0.01	-0.043	-0.055	-0.069	-0.107	-0.156	-0.253	5.236	Chaos
1.16	0.046	0	0	-0.013	-0.071	-0.088	-0.095	-0.109	-0.139	-0.188	4.465	Chaos
1.5	0	0	-0.01	-0.01	-0.047	-0.048	-0.119	-0.143	-0.157	-0.167	0	Quasi-Periodic

https://doi.org/10.1371/journal.pone.0266053.t003

Parameter *d* varying. To examine the 10-D system (1) sensitivity for the value of coefficient *d*, we let $a = 0.1$, $b = 0.1$, $c = 1.8$ and vary *d* between 0 and 1. Fig 8 gives the *LE* spectrum and *BD* of system (1) when and for initial conditions (3), it is obvious to notice the good compatibility between Lyapunov exponents spectrum and the corresponding bifurcation diagram.

When parameter *d* varies, we can see from Fig 9 that the new 10-D system (1) can exhibits periodic behavior with no complexity, chaotic behavior with one positive *LE* and a high fractional Kaplan-Yorke dimension, which implies complexity of the dynamics. In addition, higher complexity is observed when (1) generates a hyperchaotic behavior with more than one positive *LE* and higher values of Kaplan-Yorke fractal dimension. When the new system (1) generates Hyperchaotic behaviour with very high complexity where the corresponding Kaplan-Yorke fractal dimension is about 9.028 when $d = 0.02$. When the new 10-D system (1) involves into a chaotic attractor where the Kaplan-Yorke fractal dimension is about 4.667 when $d = 0.16$, 5.33 when $d = 0.85$ and may increase up to 7.937 when $d = 0.05$ indicating more complexity. When the new 10-D system (1) exhibits a quasi-periodic behavior. Various types of attractors and dynamic behaviors for special values of the parameter *d* are presented in Fig 10. Table 5 shows the *LE*, the Kaplan-Yorke fractal dimension and the dynamics for different values of *d*. To the best of the authors knowledge, this study on the new 10-D hyperchaotic system with a Kaplan-Yorke fractal dimension higher than 9 has never been studied by any researcher.

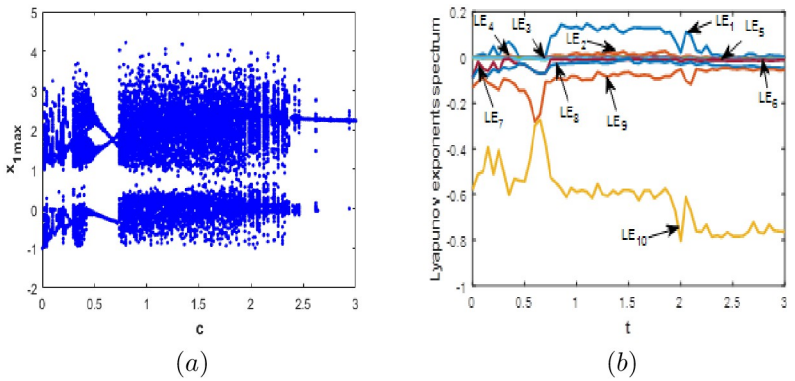

Fig 7. Bifurcation diagram (a) and Lyapunov exponents spectrum (b) of the new 10-D system (1) when: $a = 0.1$, $b = 0.1$, $d = 0.01$ and $c \in [0; 3]$.

https://doi.org/10.1371/journal.pone.0266053.g007

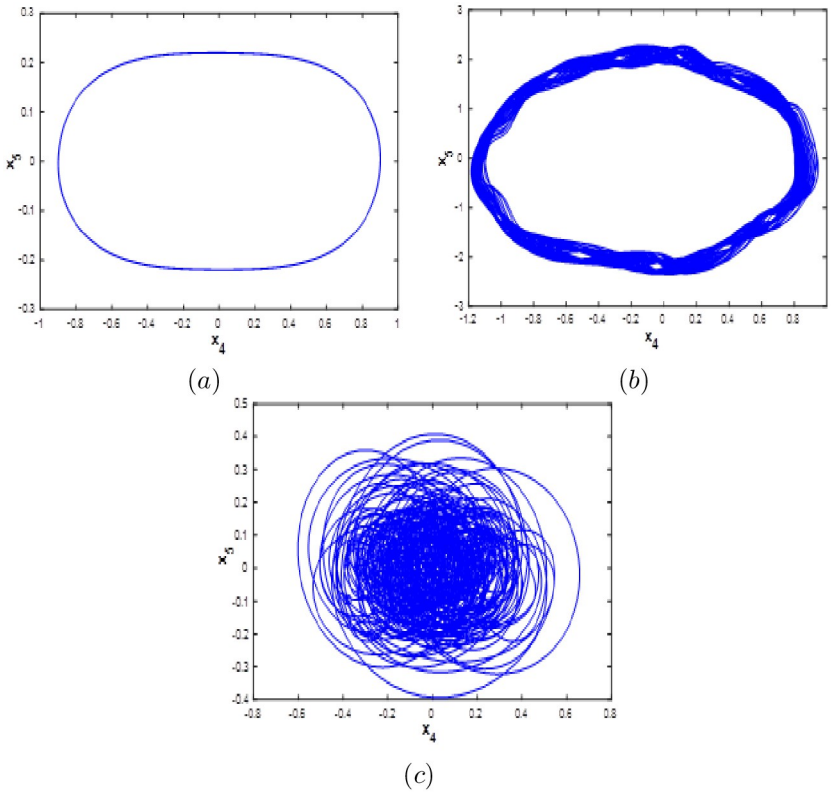

Fig 8. Phase portraits of the new 10-D system (1) for different values of *c*. (a) $x_4 - x_5$ Periodic attractor, (b) (a) $x_4 - x_5$ chaotic attractor and (c) (a) $x_4 - x_5$ hyperchaotic attractor.

https://doi.org/10.1371/journal.pone.0266053.g008

Multistability and coexisting attractors in the new 10D hyperchaotic system

To study the effect of initial criteria on the behaviour of (1), the bifurcation diagrams of (1) versus its three parameters (*a*, *b* and *c*) for six different initial conditions are calculated and plotted. The obtained bifurcation diagrams allow us to examine the phenomena of multistability; this strange occurrence demonstrates system (1)'s extraordinary sensitivity to initial conditions, which is attributable to its extremely complicated dynamics [34].

Let ξ_1, ξ_2, ξ_3, ξ_4, ξ_5 and ξ_6 be six different initial conditions for the new 10-D hyperchaotic system (1), where:

$\xi_1 = (1, 0, 0, 0, 0, 0, 0, 0, 0, 0)$ (*Bluecolour*)

Table 4. Lyapunov exponents, Kaplan-Yorke dimension and dynamics of the new 10D system (1) with parameter *c* varying.

c	LE_1	LE_2	LE_3	LE_4	LE_5	LE_6	LE_7	LE_8	LE_9	LE_{10}	D_{KY}	Dynamics
1.4	0.121	0.018	0	0	0	0	-0.010	-0.019	-0.091	-0.608	9.031	Hyperchaos
0.77	0.113	0	0	0	0	0	-0.010	-0.040	-0.107	-0.533	8.589	Chaos
0.4	0.041	0	0	0	0	-0.010	-0.024	-0.043	-0.117	-0.531	7.163	Chaos
0.1	0.025	0	0	0	0	0	-0.037	-0.072	-0.092	-0.502	6.676	Chaos
2.6	0	0	-0.010	-0.010	-0.011	-0.012	-0.014	-0.035	-0.049	-0.773	0	Quasi-Periodic

https://doi.org/10.1371/journal.pone.0266053.t004

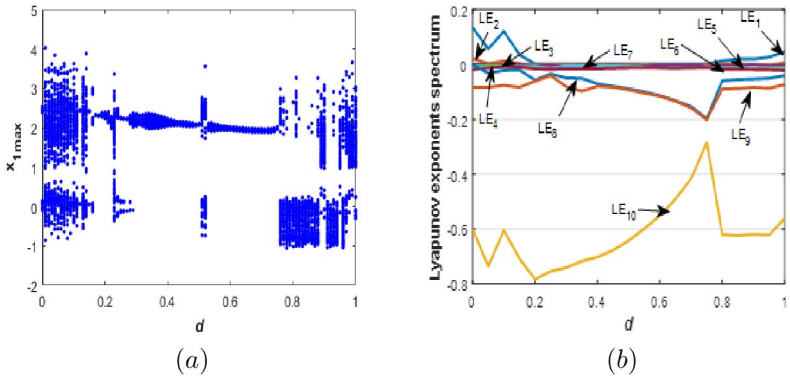

Fig 9. Bifurcation diagram (a) and Lyapunov exponents spectrum (b) of the new 10-D system (1) when: $a = 0.1$, $b = 0.1$, $c = 1.8$ and $d \in [0; 1]$.

https://doi.org/10.1371/journal.pone.0266053.g009

$\xi_2 = (0, 0, 0, 0, 0, 0, 0, 0, 0, 1)$ (*Redcolour*)

$\xi_3 = (0, 0, 0, 0, 0, 0, 0, 0, 0, -1)$ (*Greencolour*)

$\xi_4 = (0, 0, 0, 0, 0, 0, 0, 0, 0, 0.5)$ (*Magentacolour*)

$\xi_5 = (0, 0, 0, 0, 0, 0, 0, 2, 0, 0)$ (*Yellowcolour*)

$\xi_4 = (0, 0, 0, 0, 0, 0, 0, -2, 0, 0)$ (*Cyancolour*)

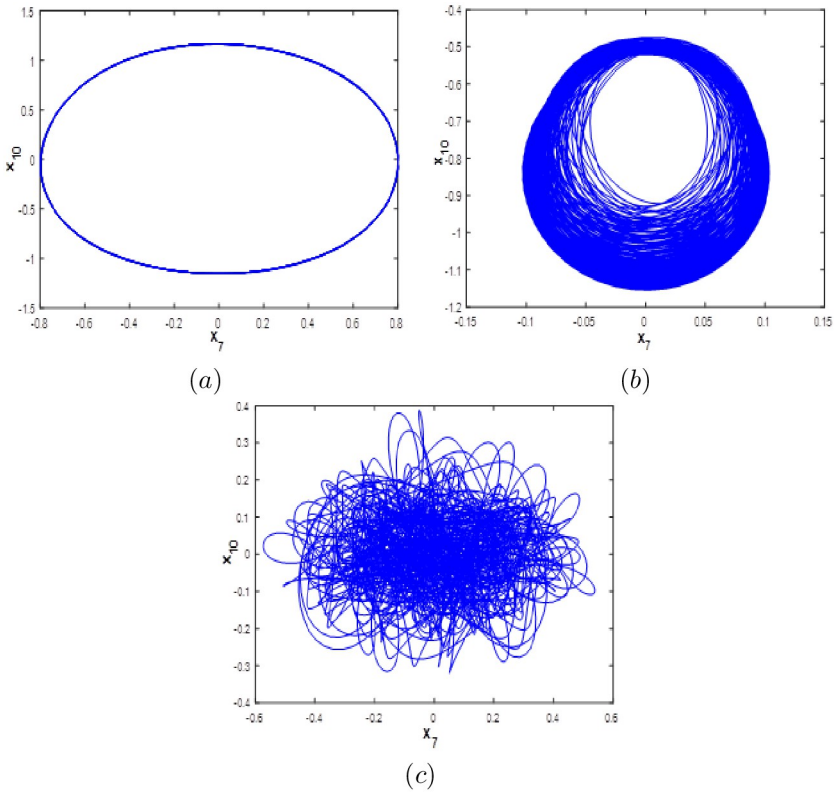

Fig 10. Phase portraits of the new 10-D system (1) for various values of *d*. (a) $x_7 - x_{10}$ Periodic attractor, (b) $x_7 - x_{10}$ chaotic attractor and (c) $x_7 - x_{10}$ hyperchaotic attractor.

https://doi.org/10.1371/journal.pone.0266053.g010

Table 5. Lyapunov exponents, Kaplan-Yorke dimension and dynamics of the new 10-D hyperchaotic system (1) with parameter *d* varying.

d	LE_1	LE_2	LE_3	LE_4	LE_5	LE_6	LE_7	LE_8	LE_9	LE_{10}	D_{KY}	Dynamics
0.02	0.111	0.019	0	0	0	0	-0.010	-0.025	-0.078	-0.599	9.028	Hyperhaos
0.05	0.056	0	0	0	0	-0.012	-0.014	-0.032	-0.083	-0.736	7.937	Chaos
0.85	0.019	0	0	0	-0.014	-0.015	-0.018	-0.055	-0.088	-0.624	5.33	Chaos
0.16	0.010	0	0	0	-0.015	-0.022	-0.023	-0.028	-0.050	-0.786	4.667	Chaos
0.5	0	0	0	0	-0.010	-0.010	-0.013	-0.089	-0.092	-0.642	0	Quasi-Periodic

https://doi.org/10.1371/journal.pone.0266053.t005

Multistability when parameter *a* varying. Here the *BD* of (1) with respect to coefficient *a* is calculated and plotted starting from six different initial points ξ_1, ξ_2, ξ_3, ξ_4, ξ_5 and ξ_6. Fix $b = 0.1$, $c = 1.8$ and $d = 0.01$, from the bifurcation diagram, it can be observed that the new 10D system (1) has six different dynamical evolutions when $a \in [0;0.2]$ as depicted in Fig 11.

When $a \in [0;0.04]$, we can see that system (1) has coexistence of one chaotic attractor starting from and five quasi-periodic attractors as shown in Fig 12(a). Coexistence of four quasi-periodic attractors starting from ξ_2, ξ_3, ξ_4 and ξ_3. and two chaotic attractors starting from ξ_1 and ξ_4 are determined when $a \in [0.05;0.02]$ as depicted in Fig 12(b). Dynamics, Kaplan-Yorke fractal dimension and Lyapunov exponents for all coexisting attractors when $a \in [0;0.2]$ are listed in Table 6.

Multistability when parameter *b* varying. Here system (1) bifurcation diagram with respect to b is calculated and plotted starting from the six different initial points ξ_1, ξ_2, ξ_3, ξ_4, ξ_5 and ξ_6. Fix $a = 0.1$, $c = 1.8$ and $d = 0.01$, from the bifurcation diagram, it can be observed that the new 10D hyperhaotic system (1) exhibit six different dynamical evolutions when $b \in [0.1;3]$ as depicted in Fig 13. When $b \in [0;1.2]$, we can see that system (1) has coexistence of

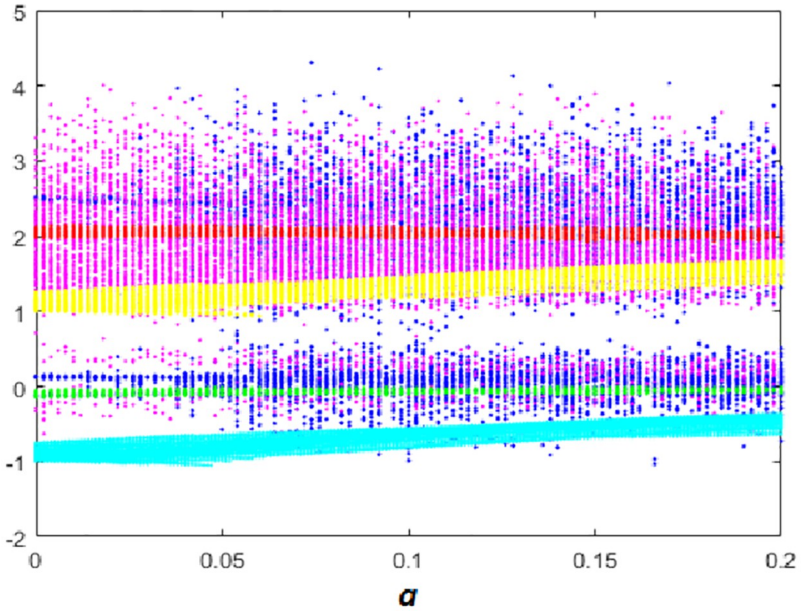

Fig 11. Bifurcation diagram of system (1) versus a starting from:ξ_1 (blue), ξ_2(red), ξ_3(green), ξ_4(magenta), ξ_5(yellow) and ξ_6(cyan).

https://doi.org/10.1371/journal.pone.0266053.g011

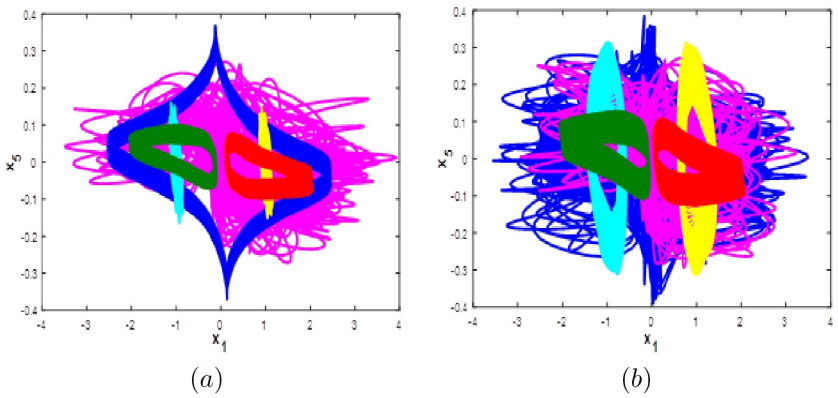

Fig 12. Coexistence of six different attractors projected on the $x_1 - x_5$ plane. (a) Coexistence of one hyperchaotic attractor and five quasi-periodic attractors when $a = 0.01$. (b) Coexistence of two hyperchaotic attractors and four quasi-periodic attractors when $a = 0.1$.

https://doi.org/10.1371/journal.pone.0266053.g012

two chaotic attractors starting from ξ_1 and ξ_4 and four periodic attractors starting from the remaining initial points as shown in Fig 14(a). Coexistence of one chaotic attractor starting from ξ_4 and five periodic attractor starting from the other initial conditions are observed when $a \in [0.13;0.19]$, (see Fig 14(b)). When $b \in [2;3]$, the new 10-D hyperchaotic system has coexistence of three chaotic attractors starting from ξ_2, ξ_3 and ξ_4 and three periodic attractors starting from ξ_1, ξ_5 and ξ_6 as shown in Fig 14(c). Dynamics, Kaplan-Yorke fractal dimension and Lyapunov exponents for all coexisting attractors when $b \in [0.1;3]$ are listed in Table 7.

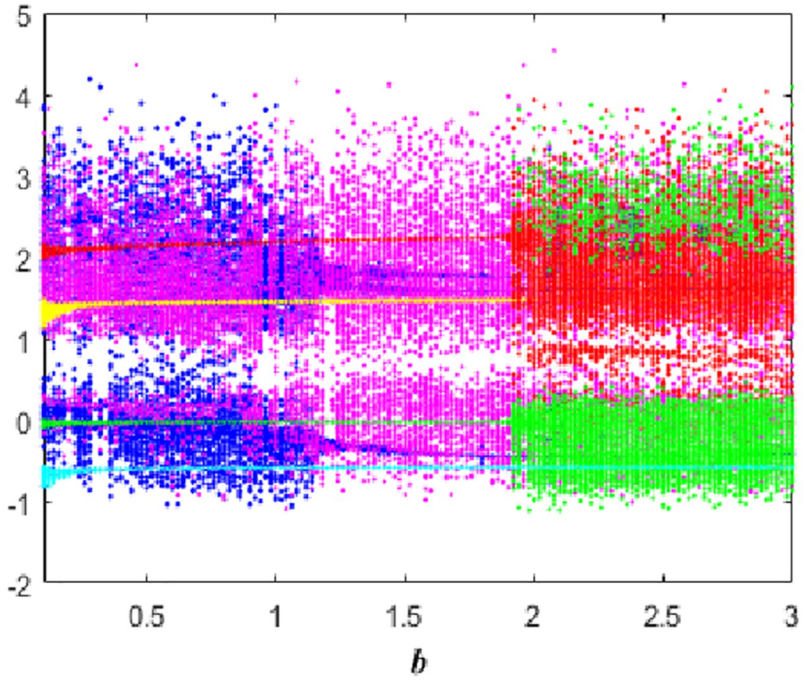

Fig 13. Bifurcation diagram of system (1) versus b starting from:ξ_1 (blue), ξ_2(red), ξ_3(green), ξ_4(magenta), ξ_5(yellow) and ξ_6(cyan).

https://doi.org/10.1371/journal.pone.0266053.g013

Table 6. Lyapunov exponents, Kaplan-Yorke dimensin and dynamics of system (1) coexisisting attractors with parameter *a* varying.

a	ξ_i	LE_1	LE_2	LE_3	LE_4	LE_5	LE_6	LE_7	LE_8	LE_9	LE_{10}	D_{KY}	Dynamics
0.01	ξ_1	0	0	0	0	-0.010	-0.012	-0.020	-0.056	-0.070	-0.693	0	Quasi-Periodic
	ξ_2, ξ_3	0	0	0	0	0	-0.010	-0.014	-0.015	-0.305	-0.355	0	Quasi-Periodic
	ξ_4	0.081	0.010	0	0	0	-0.010	-0.011	-0.021	-0.042	-0.527	9.013	Hyperchaos
	ξ_5, ξ_6	0	0	0	0	0	-0.010	-0.013	-0.138	-0.148	-0.658	0	Quasi-Periodic
0.1	ξ_1	0.129	0.024	0	0	0	0	-0.010	-0.018	0.093	-0.597	9.054	Hyperhaos
	ξ_2, ξ_3	0	0	0	0	-0.010	-0.012	-0.024	-0.026	-0.268	-0.403	0	Quais-Periodic
	ξ_4	0.089	0.014	0	0	0	0	-0.010	-0.022	-0.081	-0.533	8.876	Hyperhaos
	ξ_5, ξ_6	0	0	0	-0.010	-0.011	-0.012	-0.015	-0.143	-0.291	-0.476	0	Quais-Periodic

https://doi.org/10.1371/journal.pone.0266053.t006

Multistability when parameter *c* varying. Here the bifurcation diagram of system (1) with respect to parameter c is calculated and plotted starting from the six different initial points ξ_1, ξ_2, ξ_3, ξ_4, ξ_5 and ξ_6. Fix $a = 0.1$, $b = 0.1$ and $d = 0.01$, it can be observed from the bifurcation diagram that the new 10-D hyperchaotic system (1) exhibit six different dynamical evolutions when $c \in [0;3]$, as depicted in Fig 15. When $c \in ([0;0.4], [1.1;2.2])$, the new 10-D hyperchaotic

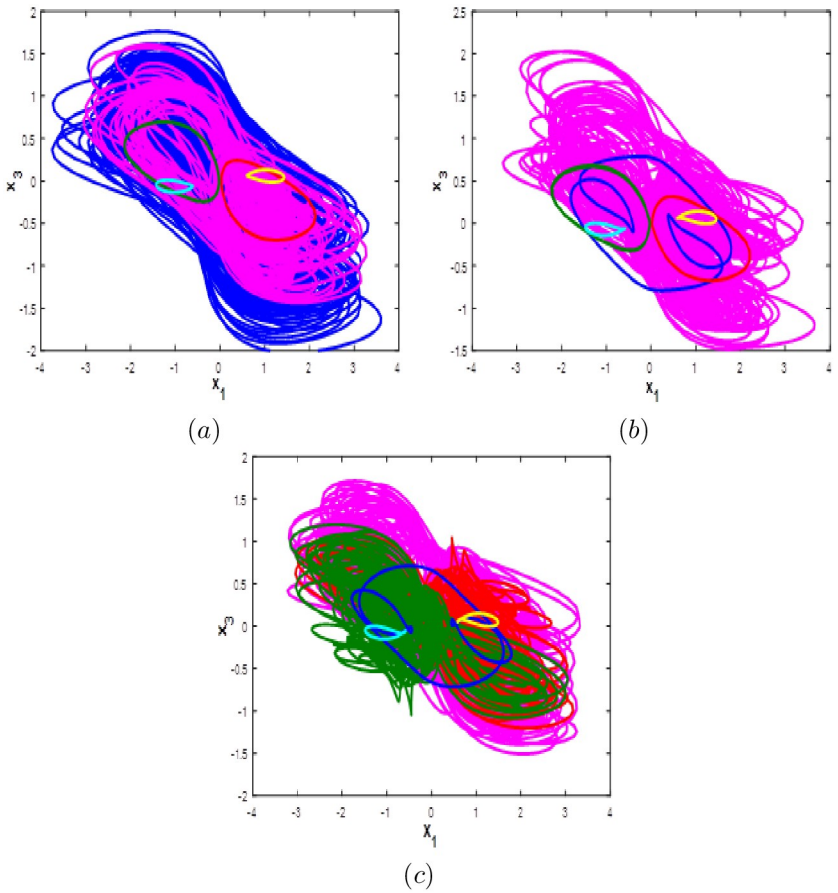

Fig 14. Coexistence of six different attractors projected on the $x_1 - x_3$ plane. (a) Coexistence of one hyperchaotic attractor (blue), one chaotic attractor (magenta) and four periodic attractors when $b = 0.5$. (b) Coexistence of one chaotic attractor and five periodic attractors when $b = 1.5$. (c) Coexistence of three chaotic attractors and three periodic attractors when $b = 2.5$.

https://doi.org/10.1371/journal.pone.0266053.g014

Table 7. Lyapunov exponents, Kaplan-Yorke dimensin and dynamics of system (1) coexisisting attractors with parameter *b* varying.

b	ξ_i	LE_1	LE_2	LE_3	LE_4	LE_5	LE_6	LE_7	LE_8	LE_9	LE_{10}	D_{KY}	Dynamics
0.5	ξ_1	0.119	0.013	0	0	-0.010	-0.032	-0.048	-0.077	-0.149	-0.424	7.545	Hyperhaos
	ξ_2, ξ_3	0	-0.010	-0.015	-0.017	-0.029	-0.032	-0.058	-0.156	-0.192	-0.325	0	Periodic
	ξ_4	0.054	0	0	-0.010	-0.024	-0.032	-0.042	-0.059	-0.121	-0.466	5.625	Chaos
	ξ_5, ξ_6	0	-0.010	-0.027	-0.030	-0.062	-0.064	-0.071	-0.103	-0.289	-0.308	0	Periodic
1.5	ξ_1	0	-0.004	-0.009	-0.010	-0.046	-0.049	-0.119	-0.144	-0.157	-0.167	0	Periodic
	ξ_2, ξ_3	0	-0.010	-0.065	-0.068	-0.076	-0.085	-0.098	-0.100	-0.194	-0.199	0	Periodic
	ξ_4	0.018	0	-0.010	-0.016	-0.051	-0.053	-0.118	-0.139	-0.156	-0.177	3.5	Chaos
	ξ_5, ξ_6	0	-0.010	-0.098	-0.099	-0.112	-0.113	-0.114	-0.133	-0.142	-0.145	0	Periodic
2.5	ξ_1	0	-0.010	-0.028	-0.031	-0.040	-0.047	-0.052	-0.140	-0.213	-0.215	0	Periodic
	ξ_2, ξ_3	0.012	0	-0.030	-0.032	-0.060	-0.061	-0.137	-0.147	-0.216	-0.220	2.4	Chaos
	ξ_4	0.017	0	-0.025	-0.027	-0.038	-0.049	-0.066	-0.145	-0.214	-0.221	2.68	Chaos
	ξ_5, ξ_6	0	-0.010	-0.045	-0.047	-0.110	-0.111	-0.113	-0.115	-0.209	-0.211	0	Periodic

https://doi.org/10.1371/journal.pone.0266053.t007

system (1) has coexistence of two chaotic and four quasi-periodic attractors as shown in Fig 16(a). Coexistence of one chaotic starting from ξ_1 and five quasi-periodic attractors is determined when $a \in ([0.5;0.7], [2.3;3])$, as depicted in Fig 16(b). Finally, when $c \in [0.8;1]$, we can observe the coexistence of one chaotic attractor starting from ξ_4 and five quasi-periodic attractors as shown if Fig 16(c).

Dynamics, Kaplan-Yorke fractal dimension and Lyapunov exponents for all coexisting attractors when $c \in [0;3]$, are listed in Table 8.

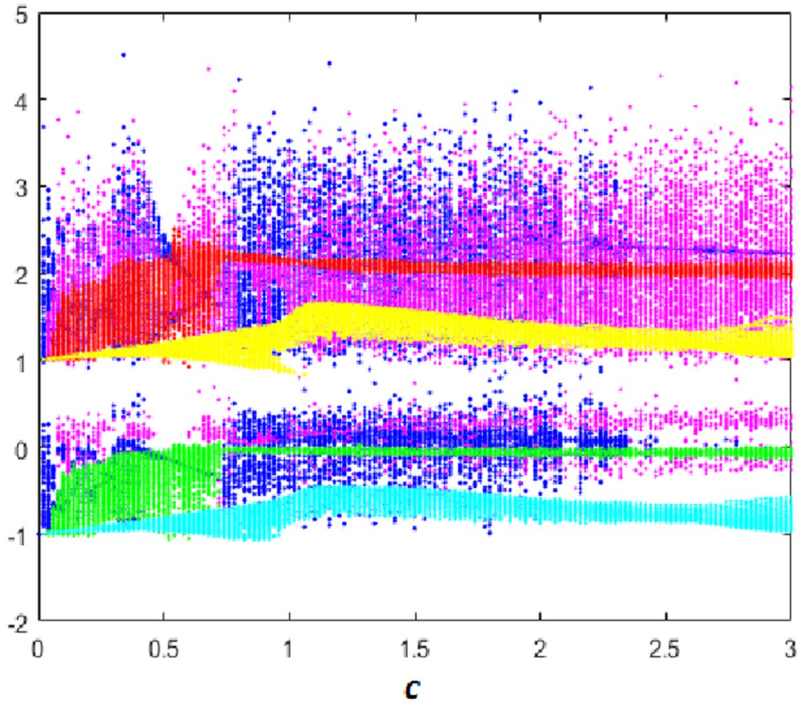

Fig 15. Bifurcation diagram of system (1) versus *c* starting from:ξ_1 (blue), ξ_2(red), ξ_3(green), ξ_4(magenta), ξ_5(yellow) and ξ_6(cyan).

https://doi.org/10.1371/journal.pone.0266053.g015

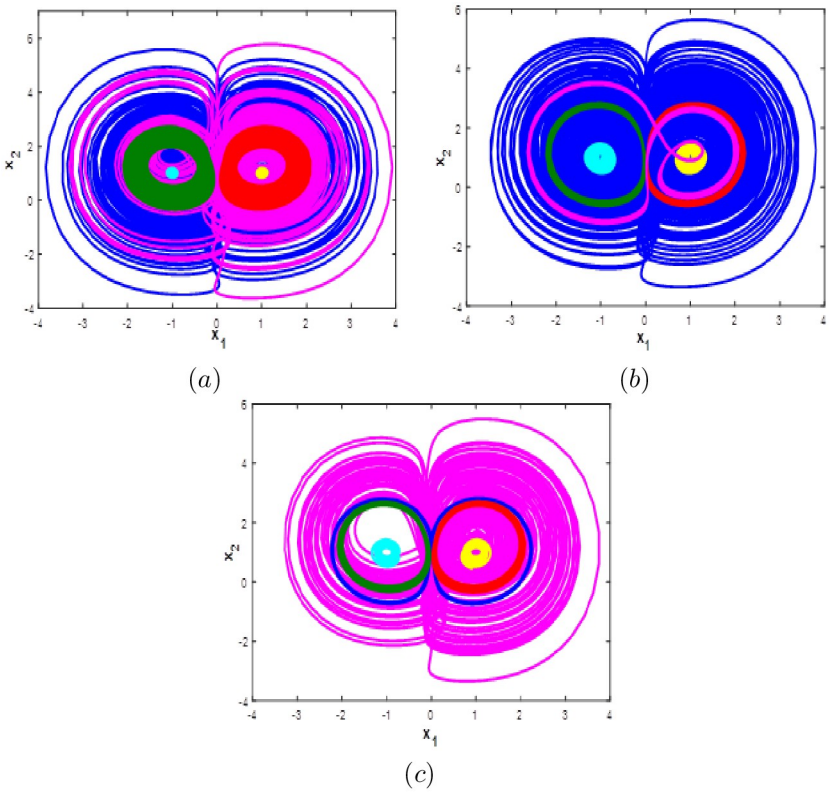

Fig 16. Coexistence of six different attractors projected on the $x_1 - x_2$ plane. (a) Coexistence of two chaotic attractor and four quasi-periodic attractors when $c = 0.3$. (b) Coexistence of one hyperchaotic attractor starting from ξ_1 (blue) and five quasi-periodic attractors when $c = 0.85$. (c) Coexistence of one chaotic attractor starting from ξ_4 (magenta), one periodic attractor (blue) and four quasi-periodic attractors when $c = 2.9$.

https://doi.org/10.1371/journal.pone.0266053.g016

Table 8. Lyapunov exponents, Kaplan-Yorke dimensin and dynamics of system (1) coexisisting attractors with parameter c varying.

c	ξ_i	LE_1	LE_2	LE_3	LE_4	LE_5	LE_6	LE_7	LE_8	LE_9	LE_{10}	D_{KY}	Dynamics
0.3	ξ_1	0.062	0	0	0	0	0	-0.010	-0.053	-0.098	-0.492	7.981	Chaos
	ξ_2, ξ_3	0	0	0	0	0	0	-0.040	-0.044	-0.203	-0.413	0	Quasi-Periodic
	ξ_4	0.032	0	0	0	0	0	-0.019	-0.045	-0.107	-0.467	7.288	Chaos
	ξ_5, ξ_6	0	0	0	0	0	-0.036	-0.039	-0.086	-0.091	-0.625	0	Quasi-Periodic
0.9	ξ_1	0.129	0.010	0	0	0	0	-0.010	-0.027	-0.101	-0.603	6.52	Hyperchaos
	ξ_2, ξ_3	0	0	0	0	-0.017	-0.021	-0.023	-0.025	-0.069	-0.607	0	Quasi-Periodic
	ξ_4	0	0	0	0	0	-0.004	-0.046	-0.083	-0.103	-0.559	0	Quasi-Periodic
	ξ_5, ξ_6	0	0	0	0	0	-0.021	-0.024	-0.112	-0.117	-0.622	0	Quasi-Periodic
2.9	ξ_1	0	-0.003	-0.006	-0.007	-0.009	-0.010	-0.014	-0.049	-0.052	-0.772	0	Periodic
	ξ_2, ξ_3	0	0	0	-0.005	-0.006	-0.008	-0.012	-0.014	-0.313	-0.364	0	Quasi-Periodic
	ξ_4	0.111	0.011	0	0	0	-0.009	-0.010	-0.017	-0.067	-0.587	9.031	Hyperchaos
	ξ_5, ξ_6	0	0	0	-0.006	-0.007	-0.010	-0.01	1 -0.088	-0.096	-0.679	0	Quasi-Periodic

https://doi.org/10.1371/journal.pone.0266053.t008

To the best of the authors knowledge, no research has been done on the new 10-D hyperchaotic chaotic system that exhibiting different coexisting attractors with the variation of its parameters.

Synchronization of the new 10D hyperchaotic system with a set of chaotic systems

This section study the synchronization of the proposed new 10-D hyperchaotic with three diverse Hyperchaotic and chaotic systems via active controllers. One considers a set of three systems as master system. The slave system will be the new 10D Hyperchaotic system. The idea is to synchronize the first three coordinates of the new 10-D hyperchaotic system with coordinates of the 3D system (17), the second three state coordinates of the new 10-D hyperchaotic system will be synchronized with the state coordinates of the 3D system (18). Finally, we will synchronize the last four coordinates of the new 10-D hyperchaotic system with the coordinates of the 4D hyeprchaotic system (19).

The first 3-D chaotic system

This subsection review the 3D chaotic system [35], which has six terms with two nonlinearities and it was given by:

$$\begin{cases} \dot{x}_{11} = e(x_{12} - x_{11}), \\ \dot{x}_{12} = x_1 x_3, \\ \dot{x}_{13} = 50 - f x_{11}^4 - g x_{13}. \end{cases} \tag{17}$$

Suppose the parameters are represented by $e = 3$, $f = 1$ and $g = 1$ and for the initial conditions (0.1; 0.1; 0.1), then, system (17) exhibits a chaotic behaviour with the following values of Lyapunov exponents: $LE_1 = 1.386$, $LE_2 = 0$, $LE_3 = -5.386$ The phase portraits of the 3D chaotic system (17) are depicted in Fig 17.

The second 3-D chaotic system

This subsection review the 3D chaotic system [36], which has three quadratic nonlinear terms. It was described as follows:

$$\begin{cases} \dot{x}_{21} = x_{22}, \\ \dot{x}_{22} = h x_{21} x_{23} + k x_{22}^2 - m x_2 - x_{22} x_{23}, \\ \dot{x}_{23} = x_{22}^2 - 1. \end{cases} \tag{18}$$

When the coefficients take the values $h = 0.1$, $k = 0.1$, $m = 0.15$ and for the initial conditions (0.2, 0.2, 0.2), system (18) exhibits a chaotic behaviour with the following values of $LE_1 = 0.053$, $LE_2 = 0$, $LE_3 = -0.183$. The phase portraits of the 3D chaotic system are presented in Fig 18.

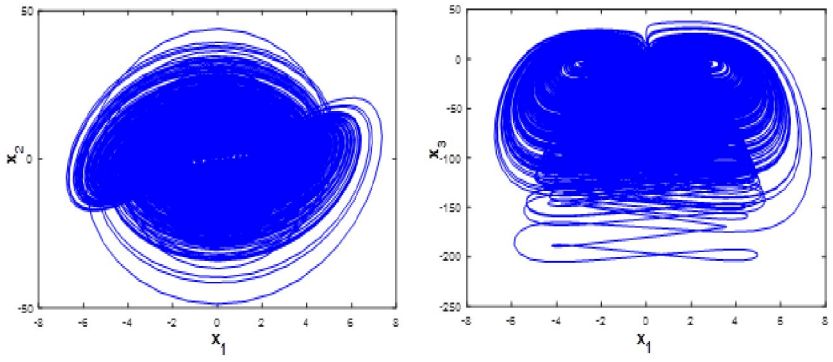

Fig 17. Phase portraits of the hyperchaotic system (17): (a) $x_1 - x_2$ attractor, (b) $x_1 - x_3$ attractor.

https://doi.org/10.1371/journal.pone.0266053.g017

The 4-D hyperchaotic system

This subsection review the 4D hyperchaotic system [37], which has four nonlinear terms and line equilibrium. It was described as follows:

$$\begin{cases} \dot{x}_{31} = x_{32} - x_{31}x_{33} - x_{32}x_{33}, \\ \dot{x}_{32} = nx_{31}x_{33} + x_{34}, \\ \dot{x}_{33} = x_{32}^2 - x_{33} + x_{34}, \\ \dot{x}_{34} = px_{32}. \end{cases} \tag{19}$$

When the parameters take the values $n = 3$, $p = -0.08$ and for the initial conditions (0.1, 0.1, 0.1, 0.1), system (12) exhibits a hyperchaotic behaviour with the following values of Lyapunov exponents $LE_1 = 0.163$, $LE_2 = 0.024$, $LE_3 = -1.823$. The phase portraits of the 4D hyperchaotic system are shown in Fig 19.

Design of active controllers for synchronization

Design of active controllers is considered in this subsection, in order to synchronize the new 10-D hyperchaotic system (1) and a set of three multidimensional systems (20). One considers

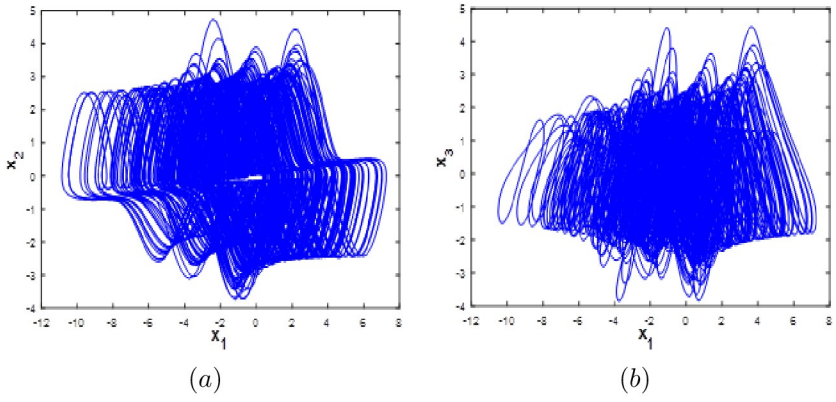

Fig 18. Phase portraits of the hyperchaotic system (18): (a) $x_1 - x_2$ attractor, (b) $x_1 - x_3$ attractor.

https://doi.org/10.1371/journal.pone.0266053.g018

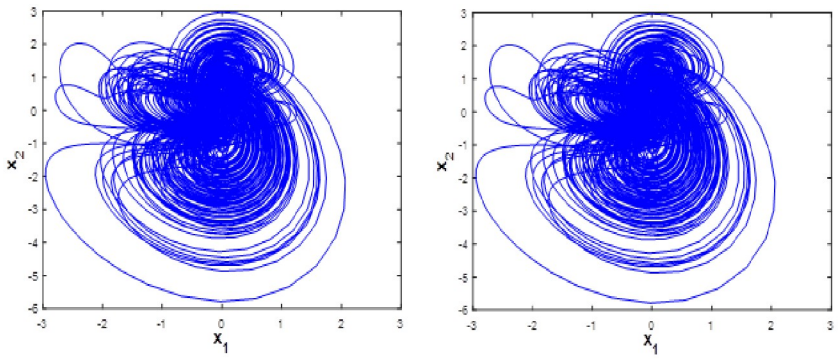

Fig 19. Phase portraits of the hyperchaotic system (19): (a) $x_1 - x_2$ attractor, (b) $x_1 - x_3$ attractor.

https://doi.org/10.1371/journal.pone.0266053.g019

the following set of chaotic systems (The first 3D chaotic system (17), the second 3D chaotic system (18) and the 4D hyperchaotic system (19) as master system:

$$\begin{cases} \dot{x}_{11} = e(x_{12} - x_{11}), \\ \dot{x}_{12} = x_1 x_3, \\ \dot{x}_{13} = 50 - f x_{11}^4 - g x_{13}, \\ \dot{x}_{21} = x_{22}, \\ \dot{x}_{22} = h x_{21} x_{23} + k x_{22}^2 - m x_2 - x_{22} x_{23}, \\ \dot{x}_{23} = x_{22}^2 - 1, \\ \dot{x}_{31} = x_{32} - x_{31} x_{33} - x_{32} x_{33}, \\ \dot{x}_{32} = n x_{31} x_{33} + x_{34}, \\ \dot{x}_{33} = x_{32}^2 - x_{33} + x_{34}, \\ \dot{x}_{34} = p x_{32}. \end{cases} \tag{20}$$

Then, the new 10-D system is studied as a master system and described as follows:

$$\begin{cases} \dot{x_1} = x_3 + x_1 x_2 - x_1 + u_1, \\ \dot{x_2} = 1 + a(x_2 - x_1^4) - x_1^2 + u_2, \\ \dot{x_3} = -x_1 + x_3 + x_4 + u_3, \\ \dot{x_4} = -b x_3 + c x_5 + u_4, \\ \dot{x_5} = -x_4 + x_6 + u_5, \\ \dot{x_6} = -x_5 + x_7 + u_6, \\ \dot{x_7} = -x_6 + x_8 + u_7, \\ \dot{x_8} = -x_7 + (1 - d) x_9 + u_8, \\ \dot{x_9} = -x_8 + x_{10} + u_9, \\ \dot{x}_{10} = -x_9 + x_7 + u_{10}, \end{cases} \tag{21}$$

where the functions of the active control to be found is u_1, u_2, u_3, u_4, u_5, u_6, u_7, u_8, u_9 and u_{10}. The state errors are defined as $e - 1 = x_1 - x_{11}$, $e_2 = x_2 - x_{12}$, $e_3 = x_3 - x_{13}$, $e_4 = x_4 - x_{21}$, $e_5 = x_5 - x_2$, $e_6 = x_6 - x_{23}$, $e_7 = x_7 - x_{31}$, $e_8 = x_8 - x_{32}$, $e_9 = x_9 - x_{33}$, $e_{10} = x_{10} - x_{34}$ From the slave system (21), we subtract master system (20) including the control functions, thus, we obtain error system as follows:

$$\begin{cases} \dot{e_1} = \dot{x_1} - \dot{x_{11}} = x_3 + x_1x_2 - x_1 - e(x_{12} - x_{11}) + u_1, \\ \dot{e_2} = \dot{x_2} - \dot{x_{12}} = 1 + a(x_2 - x_1^4) - x_1^2 - x_1x_3 + u_2, \\ \dot{e_3} = \dot{x_3} - \dot{x_{13}} = -x_1 + x_3 + x_4 - 50 + fx_{11}^4 + gx_{13} + u_3, \\ \dot{e_4} = \dot{x_4} - \dot{x_{21}} = -bx_3 + cx_5 - x_{22} + u_4, \\ \dot{e_5} = \dot{x_5} - \dot{x_{22}} = -x_4 + x_6 - hx_{21}x_{23} - kx_{22}^2 + mx_2 + x_{22}x_{23} + u_5, \\ \dot{e_6} = \dot{x_6} - \dot{x_{23}} = -x_5 + x_7 - x_{22}^2 + 1 + u_6, \\ \dot{e_7} = \dot{x_7} - \dot{x_{31}} = -x_6 + x_8 - x_{32} + x_{31}x_{33} + x_{32}x_{33} + u_7, \\ \dot{e_8} = \dot{x_8} - \dot{x_{32}} = -x_7 + (1 - d)x_9 - nx_{31}x_{33} - x_{34} + u_8, \\ \dot{e_9} = \dot{x_9} - \dot{x_{33}} = -x_8 + x_{10} - x_{32}^2 + x_{33} - x_{34} + u_9, \\ \dot{e}_{10} = \dot{x_{10}} - \dot{x_{34}} = -x_9 + x_7 - px_{32} + u_{10}. \end{cases} \tag{22}$$

Our aim is to design the active control functions, which control the error system to be asymptotically stable; in order to ascertain synchronization between the new 10-D hyperchaotic system (21) and set of systems (20).

By choosing the active control functions as the follows:

$$\begin{cases} u_1 = e(x_{12} - x_{11}) - x_3 - x_1x_2 - e_1, \\ u_2 = x_1x_3 - 1 - a(x_2 - x_1^4) + x_1^2 - e_2, \\ u_3 = 50 - fx_{11}^4 - gx_{13} + x_1 - x_3 - x_4 - e_3, \\ u_4 = x_{22} + bx_3 - cx_5 + bx_3 - cx_5 - e_4, \\ u_5 = hx_{21}x_{23} + kx_{22}^2 - mx_2 - x_{22}x_{23} + x_4 - x_6 - e_5, \\ u_6 = x_{22}^2 - 1 + x_5 - x_7 - e_6, \\ u_7 = x_{32} - x_{31}x_{33} - x_{32}x_{33} + x_6 - x_8 - e_7, \\ u_8 = nx_{31}x_{33} + x_{34} + x_7 - (1 - d)x_9 - e_8, \\ u_9 = x_{32}^2 - x_{33} + x_{34} + x_8 - x_{10} - e_9, \\ u_{10} = px_{32} + x_9 - x_7 - e_{10}. \end{cases} \tag{23}$$

The dynamical equations of error system becomes:

$$\begin{cases} \dot{e_1} = -e_1, \\ \dot{e_2} = -e_2, \\ \dot{e_3} = -e_3, \\ \dot{e_4} = -e_4, \\ \dot{e_5} = -e_5, \\ \dot{e_6} = -e_6, \\ \dot{e_7} = -e_7, \\ \dot{e_8} = -e_8, \\ \dot{e_9} = -e_9, \\ \dot{e}_{10} = -e_{10}. \end{cases} \tag{24}$$

It can be noted from (24) that after applying the proposed active control functions (23) the error system becomes linear with the following state representation:

$$\begin{bmatrix} \dot{e}_1 \\ \dot{e}_2 \\ \dot{e}_3 \\ \dot{e}_4 \\ \dot{e}_5 \\ \dot{e}_6 \\ \dot{e}_7 \\ \dot{e}_8 \\ \dot{e}_9 \\ \dot{e}_{10} \end{bmatrix} = \begin{bmatrix} -1 & 0 & 0 & 0 & 0 & 0 & 0 & 0 & 0 & 0 \\ 0 & -1 & 0 & 0 & 0 & 0 & 0 & 0 & 0 & 0 \\ 0 & 0 & -1 & 0 & 0 & 0 & 0 & 0 & 0 & 0 \\ 0 & 0 & 0 & -1 & 0 & 0 & 0 & 0 & 0 & 0 \\ 0 & 0 & 0 & 0 & -1 & 0 & 0 & 0 & 0 & 0 \\ 0 & 0 & 0 & 0 & 0 & -1 & 0 & 0 & 0 & 0 \\ 0 & 0 & 0 & 0 & 0 & 0 & -1 & 0 & 0 & 0 \\ 0 & 0 & 0 & 0 & 0 & 0 & 0 & -1 & 0 & 0 \\ 0 & 0 & 0 & 0 & 0 & 0 & 0 & 0 & -1 & 0 \\ 0 & 0 & 0 & 0 & 0 & 0 & 1 & 0 & 0 & -1 \end{bmatrix} \begin{bmatrix} e_1 \\ e_2 \\ e_3 \\ e_4 \\ e_5 \\ e_6 \\ e_7 \\ e_8 \\ e_9 \\ e_{10} \end{bmatrix} \tag{25}$$

It is easy to check that all eigenvalues of the states matrix (25) are negatives, so, based on Routh-Hurwitz condition; the error system is stable which assure synchronization between the slave system (21) and master system (20). So, the designed active functions ensure that the first three states of the 10 D system will be synchronized with the states of the first chaotic system (17). The second three states of the new 10-D hyperchaotic system will be synchronized with the states of second chaotic system (18) and the last four states of the new 10-D hyperchaotic system will be synchronized with the states of the 4D hyperchaotic system (19).

Simulation results

For numerical simulations the initial conditions of the master system (10) are chosen as: (0.1, 0.1, 0.1, 0.2, 0.2, 0.2, 0.1, 0.1, 0.1, 0.1) The parameters of the master system are chosen as: $e = 3$, $f = 1$, $g = 1$, $h = 0.$, $k = 0.1$, $m = 0.15$, $n = 3$ and $p = -0.08$ The initial conditions of the slave system (10) are chosen as (1, 1, 1, 1, 1, 1, 1, 0, 0, 0) The parameters of the slave system are chosen as: $a = 0.1$, $b = 0.1$, $c = 1.8$ and $d = 0$. Active controllers is switched on at $t = 200s$ and all the states error time evolution are depicted in Fig 20. The results shows that all the ten states of error system (22) evolve chaotically with time when the active controllers are deactivated (when $t < 200s$) indicating non synchronization. After that (when $t \geq 200s$), the controllers are activated and it can be seen that all the states synchronization error converge rapidly to zero. So, simulation results showing the success of the proposed active controllers (23) to synchronize the new 10D hyperchaotic system with a class of three multidimensional chaotic and

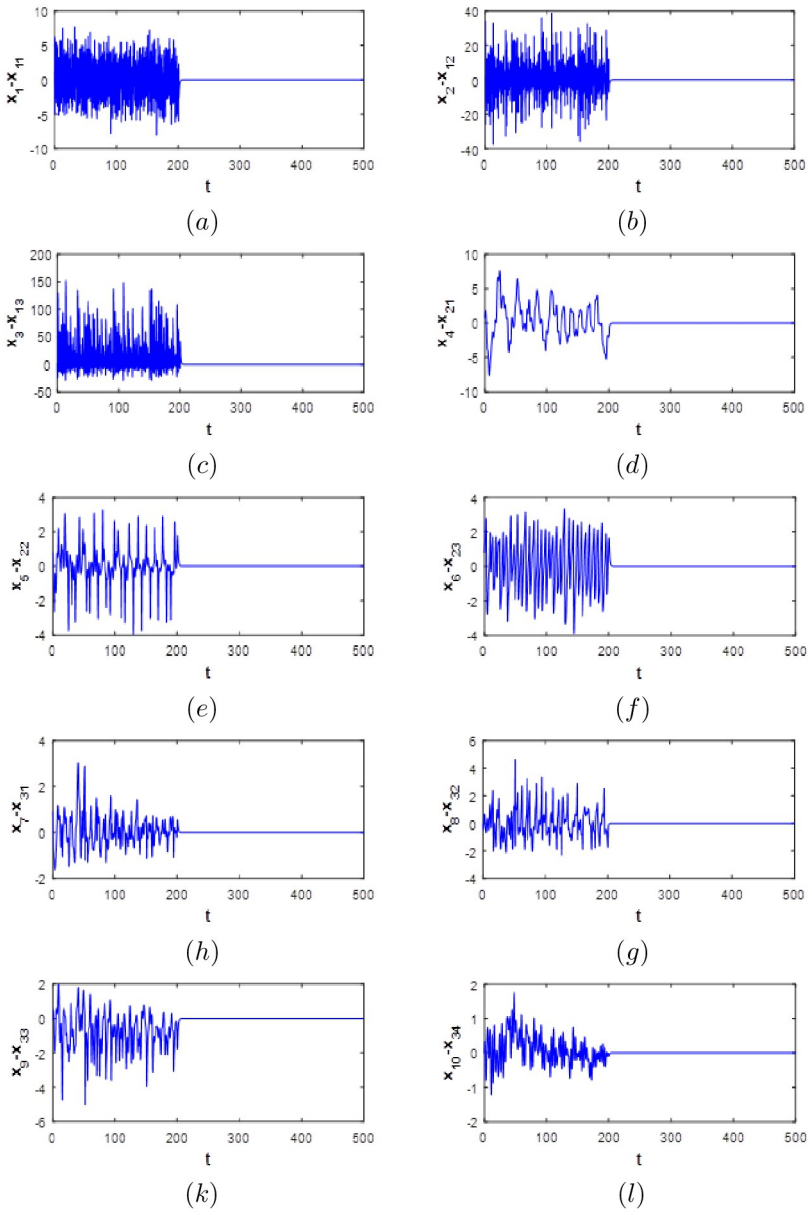

Fig 20. Time evolution of the synchronization errors with controllers deactivated ($t < 200s$) and activated ($t > 200s$).

https://doi.org/10.1371/journal.pone.0266053.g020

hyperchaotic systems. To the best of the authors knowledge, no study has been done to investigates the synchronization of the new 10D hyperchaotic system with the active control strategy. Also, synchronization of the proposed 10D system (1) with a class of low dimensional systems making it very desirable to use in secure communications schemes that need high complexity.

Circuit implementation of the new 10-D system

In order to test system (1) physical feasibility, an equivalent electronic circuit for the new 10-D hyperchaotic system (1) is developed using Multisim 13.0 software as depicted in Fig 21. Using

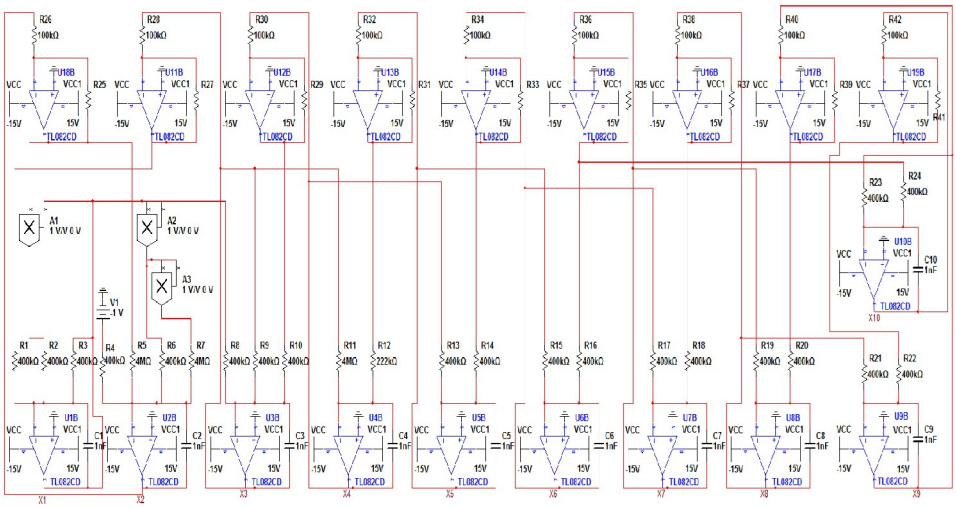

Fig 21. Electronic circuit schematic of the proposed 10-D hyperchaotic system (1).

https://doi.org/10.1371/journal.pone.0266053.g021

the Kirchhoff's laws to the circuit in Fig 21, the circuital equations of the new 10D Hyperchaotic system (1) becomes:

$$\begin{cases} \dot{x}_1 = \frac{1}{R_1C_1}x_3 - \frac{1}{R_2C_1}x_1x_2 - \frac{1}{R_3C_1}x_1, \\ \dot{x}_2 = \frac{1}{R_4C_2}V + \frac{1}{R_5C_2}x_2 - \frac{1}{R_6C_2}x_1^2 - \frac{1}{R_7C_2}x_1^4, \\ \dot{x}_3 = -\frac{1}{R_8C_3}x_1 - \frac{1}{R_9C_3}x_3 + \frac{1}{R_{10}C_3}x_4, \\ \dot{x}_4 = -\frac{1}{R_{11}C_4}x_3 + \frac{1}{R_{12}C_4}x_5, \\ \dot{x}_5 = -\frac{1}{R_{13}C_5}x_4 + \frac{1}{R_{14}C_5}x_6, \\ \dot{x}_6 = -\frac{1}{R_{15}C_6}x_5 + \frac{1}{R_{16}C_6}x_7, \\ \dot{x}_7 = -\frac{1}{R_{17}C_7}x_6 + \frac{1}{R_{18}C_7}x_8, \\ \dot{x}_8 = -\frac{1}{R_{19}C_8}x_7 + \frac{1}{R_{20}C_8}x_9, \\ \dot{x}_9 = -\frac{1}{R_{21}C_9}x_8 + \frac{1}{R_{22}C_9}x_{10}, \\ \dot{x}_{10} = -\frac{1}{R_{23}C_{10}}x_9 + \frac{1}{R_{27}C_{10}}x_7. \end{cases} \tag{26}$$

By using TL082CD operational amplifiers, the circuit would have nine reversers and ten integrators, also this study considered three multipliers IC AD633. All active devices have a supply voltage $\pm 15V$. The values of circuital components are selected as follows: $R_1 = R_2 = R_3 = R_4 = R_6 = R_8 = R_9 = R_{10} = 400K\Omega$, $R_5 = R_7 = R_{11} = 4M\Omega$, $R_{12} = 222.23K\Omega$, $R_{20} = 404.04K\Omega$, $R_i =$

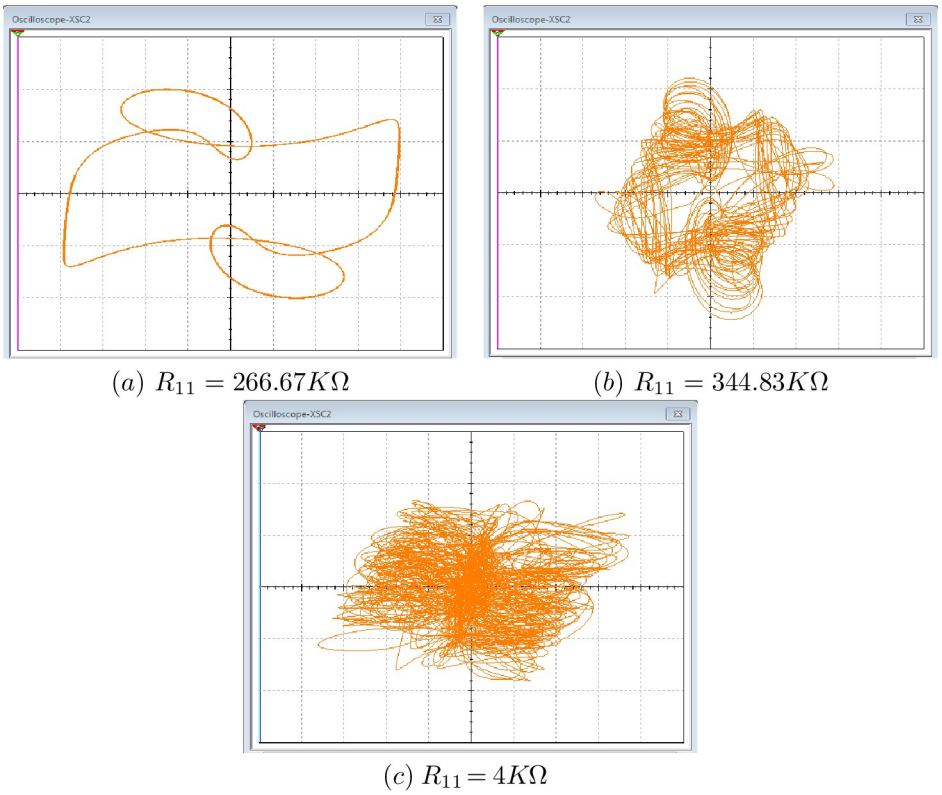

Fig 22. Experimental phase portraits of the system (1) $x_3 - x_4$ plane. (a): Periodic orbit, (b): Chaotic attractor and (c): Hyperchaotic attractor.

https://doi.org/10.1371/journal.pone.0266053.g022

$400K\Omega$ for $i = 13, \ldots, 19$ and $i = 21, \ldots, 24$, $R_i = 100K\Omega$ for $i = 25, \ldots, 42$, and $C_i = 1nf$ for $i = 1, \ldots, 10$.

Fig 22(a)–22(c) shows the periodic attractor, the chaotic attractor and the hyperchaotic attractor respectively derived by Multisim 13.0. It can be noticed that the Multisim 13.0 simulation results are akin to the Matlab results depicted in Fig 6(a)–6(c) which confirm the proposed 10-D system (1) physical feasibility.

Fig 23 shows four coexistence attractors obtained from the Multisim 13.0 based implementation of the 10-D system (1) for similar values of coefficients $a = b = 0.1$, $c = 1.8$, $d = 0.01$ and four different initial conditions ξ_1, ξ_2, ξ_3 and ξ_4

Fig 23(a)–23(d) shows respectively good compatibility with the four coexisting attractors (the magenta chaotic attractor, the red chaotic attractor, the green chaotic attractor and the blue periodic attractor) depicted in Fig 14(c) using Matlab software. These results confirm the physical existence of the coexisting attractors in the proposed 10-D system (1).

Conclusion

In this work, a new ten-dimensional hyperchaotic system is first presented; the new system contains four positive parameters and twenty-three terms with two quadratic and a quartic nonlinearities. The new system has many specifics properties, it has three unstable equilibrium points, it can exhibits four different dynamical behaviours (periodic, quasi-periodic, chaos and hyperchaos) for special values of parameters. In addition, the new system may generate many

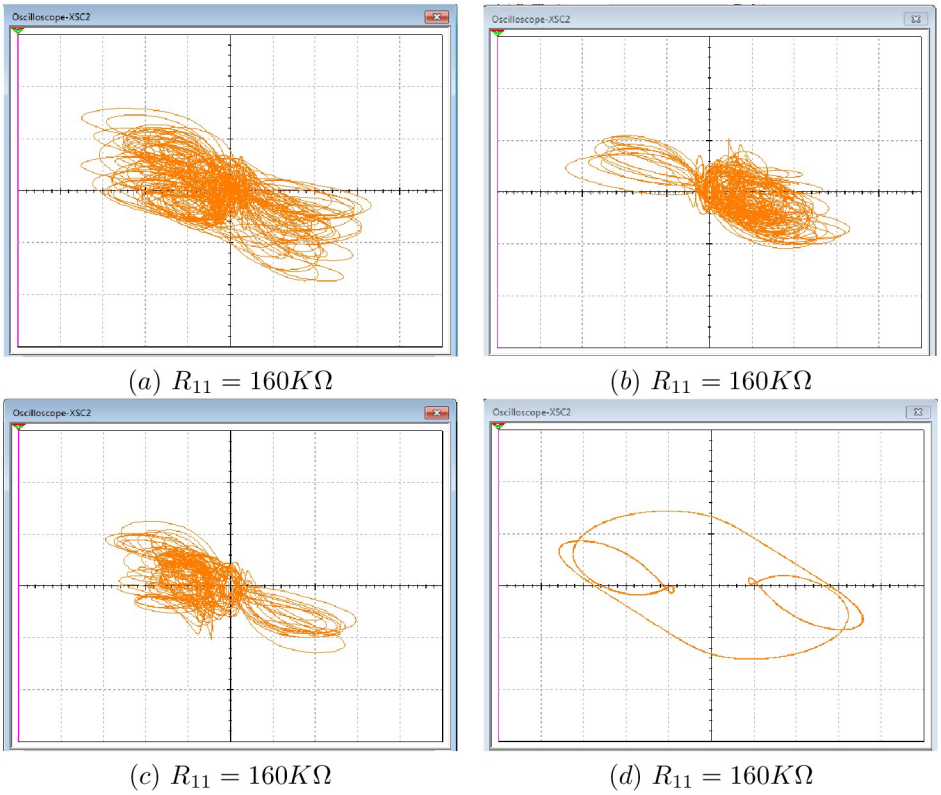

Fig 23. Experimental phase portraits of four coexisting attractors: (a), (b) and (c) three chaotic attractors with initial points (0,0,0,0,0,0,0,0,0,0.5), (0,0,0,0,0,0,0,0,0,±1); (d) periodic attractor with initial point (1,0,0,0,0,0,0,0,0,0).

https://doi.org/10.1371/journal.pone.0266053.g023

coexisting attractors with high fractal dimension when fixing the parameters and changing the initial conditions. Dynamical properties of the new system is investigated using Lyapunov exponents, Kaplan-Yorke dimension, bifurcation diagrams, phase portraits, equilibrium points stability and dissipativity. The idea of synchronizing the new 10-D high dimensional system with a set of three low dimensional system is applied by using active controllers; which guarantee the convergence of the synchronization errors to zero asymptotically. Finally, in order to prove the real feasibility of the new system and the physical existence of the coexisting attractor, an equivalent electronic circuit was designed using Multisim. The obtained results show a good agreement with Matlab results, which confirm the feasibility of both the 10-D system and its dynamical behaviours. We strongly believe that the new 10-D Hyperchaotic system with its high dimension, very complex dynamic and easy to implement circuit schematic can be applied in various chaotic-based applications. The hardware implementations of the new systems along with their applications are considered as the future direction of the work.

Acknowledgments

The authors are grateful to all reviewers for their important comments and suggestions which has helped increase the quality of the paper. This work was supported by the Center of Research Excellence, Incubation Management Center, Universiti Sultan Zainal Abidin, Malaysia.

Author Contributions

Conceptualization: Khaled Benkouider, Muhammad Zaini Ahmad.

Data curation: Badis Lekouaghet.

Formal analysis: Khaled Benkouider, Mohd Asrul Hery Ibrahim, Muhammad Zaini Ahmad.

Funding acquisition: Mohamad Afendee Mohamed, Mohd Asrul Hery Ibrahim.

Investigation: Khaled Benkouider, Muhammad Zaini Ahmad.

Methodology: Khaled Benkouider, Toufik Bouden, Badis Lekouaghet.

Resources: Aceng Sambas, Mohamad Afendee Mohamed.

Supervision: Toufik Bouden, Mohamad Afendee Mohamed, Mustafa Mamat, Mohd Asrul Hery Ibrahim, Muhammad Zaini Ahmad.

Validation: Khaled Benkouider, Toufik Bouden, Aceng Sambas, Badis Lekouaghet, Mohamad Afendee Mohamed, Sulaiman Ibrahim Mohammed, Mustafa Mamat, Mohd Asrul Hery Ibrahim, Muhammad Zaini Ahmad.

Visualization: Khaled Benkouider, Aceng Sambas, Badis Lekouaghet, Sulaiman Ibrahim Mohammed.

Writing – original draft: Khaled Benkouider, Muhammad Zaini Ahmad.

Writing – review & editing: Toufik Bouden, Aceng Sambas, Badis Lekouaghet, Mohamad Afendee Mohamed, Sulaiman Ibrahim Mohammed, Mustafa Mamat, Mohd Asrul Hery Ibrahim, Muhammad Zaini Ahmad.

References

1. Conant G., Wolfe K. Turning a hobby into a job: how duplicated genes find new functions. Nat. Rev. Genet. 2008, 9, 938–950. https://doi.org/10.1038/nrg2482 PMID: 19015656
2. Benkouider K, Halimi M, Bouden T. Secure communication scheme using chaotic time-varying delayed system. Int. J. Comput. Appl. Technol. 2019 Dec; 60(2):175. https://doi.org/10.1504/IJCAT.2019.10021785
3. Sambas A., Vaidyanathan S., Tlelo-Cuautle E., Abd-El-Atty B., Abd El-Latif A. A., Guillén-Fernández O, et al. A 3-D multi-stable system with a peanut-shaped equilibrium curve: Circuit design, FPGA realization, and an application to image encryption. IEEE Access, 2020, 8, 137116–137132. https://doi.org/10.1109/ACCESS.2020.3011724
4. Benkouider K., Bouden T., Sambas A., Mohamed M. A., Sulaiman I. M., Mamat M, et al. Dynamics, Control and Secure Transmission Electronic Circuit Implementation of a New 3D Chaotic System in Comparison With 50 Reported Systems. IEEE Access, 2021, 9, 152150–152168. https://doi.org/10.1109/ACCESS.2021.3126655
5. Zhou L, Tan F. A chaotic secure communication scheme based on synchronization of double-layered and multiple complex networks. Nonlinear Dyn. 2019; 96(2).869–883. https://doi.org/10.1007/s11071-019-04828-7
6. Silva-Juárez A., Tlelo-Cuautle E., de la Fraga L. G., Li R. Optimization of the Kaplan-Yorke dimension in fractional-order chaotic oscillators by metaheuristics. Applied Mathematics and Computation, 2021, 294, 125831. https://doi.org/10.1016/j.amc.2020.125831
7. Vaidyanathan S., He S., Sambas A. A new multistable double-scroll 4-D hyperchaotic system with no equilibrium point, its bifurcation analysis, synchronization and circuit design. Archives of Control Sciences, 2021, 31(1), 99–128.
8. Singh J. P., Rajagopal K., Roy B. K. A new 5D hyperchaotic system with stable equilibrium point, transient chaotic behaviour and its fractional-order form. Pramana, 2018, 91(3), 1–10. https://doi.org/10.1007/s12043-018-1599-9
9. Alattas K. A., Mostafaee J., Sambas A., Alanazi A. K., Mobayen S., Zhilenkov A. Nonsingular Integral-Type Dynamic Finite-Time Synchronization for Hyper-Chaotic Systems. Mathematics, 2022, 10(1), 115. https://doi.org/10.3390/math10010115

10. Lagmiri SN, Amghar M, Sbiti N. Seven Dimensional New Hyperchatic Systems: Dynamics and Synchronization by a High Gain Observer Design. Int J. Control and Automation. 2017, 10(1).251–266. https://doi.org/10.14257/ijca.2017.10.1.23

11. Kang S., Liang Y., Wang Y., VI M. Color image encryption method based on 2D-variational mode decomposition. Multimedia Tools and Applications, 2019, 78(13), 17719–17738. https://doi.org/10.1007/s11042-018-7129-4

12. Zhu JL, Dong J, Gao HQ. Nine-Dimensional Eight-Order Chaotic System and its Circuit Implementation. Applied Mechanics and Materials. 2014, 716-717. 1346–1351.

13. Mahmoud EE, Abualnaja KM, Althagafi OA. High dimensional, four positive Lyapunov exponents and attractors with four scroll during a new hyperchaotic complex nonlinear model. AIP Advances. American Institute of Physics Inc. 2018, 8(6). 065018.

14. Mahmoud EE, Higazy M, Al-Harthi TM. A New Nine-Dimensional Chaotic Lorenz System with Quaternion Variables: Complicated Dynamics, Electronic Circuit Design, Anti-Anticipating Synchronization, and Chaotic Masking Communication Application. Mathematics. MDPI AG. 2019 Aug; 7(10). 877. https://doi.org/10.3390/math7100877

15. Jianliang Z, Shouqiang K, Huaqiang G, Yujing W. Ten-dimensional nine-order chaotic system and its circuit implementation. in 2015 IEEE 12th International Conference on Electronic Measurement and Instruments, ICEMI 2015. Institute of Electrical and Electronics Engineers Inc. 2015, 964–968.

16. Yu F., Liu L., He B., Huang Y., Shi C., Cai S., et al. Analysis and FPGA realization of a novel 5D hyperchaotic four-wing memristive system, active control synchronization, and secure communication application. Complexity, 2019, 4047957. https://doi.org/10.1155/2019/4047957

17. Zambrano-Serrano E., Anzo-Hernández A. A novel antimonotic hyperjerk system: Analysis, synchronization and circuit design. Physica D: Nonlinear Phenomena, 2021, 424, 132927. https://doi.org/10.1016/j.physd.2021.132927

18. Munoz-Pacheco J. M., Posadas-Castillo C., Zambrano-Serrano E. The effect of a non-local fractional operator in an asymmetrical glucose-insulin regulatory system: analysis, synchronization and electronic implementation. Symmetry, 2020, 12(9), 1395. https://doi.org/10.3390/sym12091395

19. Vaidyanathan S., Sambas A., Abd-El-Atty B., Abd El-Latif A. A., Tlelo-Cuautle E., Guillén-Fernández O., et al. A 5-D multi-stable hyperchaotic two-disk dynamo system with no equilibrium point: Circuit design, FPGA realization and applications to TRNGs and image encryption. IEEE Access, 2021, 9, 81352–81369. https://doi.org/10.1109/ACCESS.2021.3085483

20. Vaidyanathan S., Moroz I. M., El-Latif A. A. A., Abd-El-Atty B., Sambas A. A new multistable jerk system with Hopf bifurcations, its electronic circuit simulation and an application to image encryption. International Journal of Computer Applications in Technology, 2021, 67(1), 29–46. https://doi.org/10.1504/IJCAT.2021.10044864

21. Nazari M., Mehrabian M. A novel chaotic IWT-LSB blind watermarking approach with flexible capacity for secure transmission of authenticated medical images. Multimedia Tools and Applications, 2021, 80 (7), 10615–10655. https://doi.org/10.1007/s11042-020-10032-2

22. Trujillo-Toledo D. A., López-Bonilla O. R., García-Guerrero E. E., Tlelo-Cuautle E., López-Mancilla D., Guillén-Fernández O., et al. Real-time RGB image encryption for IoT applications using enhanced sequences from chaotic maps. Chaos, Solitons and Fractals, 2021, 153, 111506. https://doi.org/10.1016/j.chaos.2021.111506

23. Hemdan E. E. D. An efficient and robust watermarking approach based on single value decompression, multi-level DWT, and wavelet fusion with scrambled medical images. Multimedia Tools and Applications, 2021, 80(2), 1749–1777. https://doi.org/10.1007/s11042-020-09769-7

24. García-Guerrero E. E., Inzunza-González E., López-Bonilla O. R., Cárdenas-Valdez J. R., Tlelo-Cuautle E. Randomness improvement of chaotic maps for image encryption in a wireless communication scheme using PIC-microcontroller via Zigbee channels. Chaos, Solitons and Fractals, 2020, 133, 1096468. https://doi.org/10.1016/j.chaos.2020.109646

25. Silva-Juárez A., Tlelo-Cuautle E., De La Fraga L. G., Li R. FPAA-based implementation of fractional-order chaotic oscillators using first-order active filter blocks. Journal of advanced research, 2020, 25, 77–85. https://doi.org/10.1016/j.jare.2020.05.014 PMID: 32922976

26. Tlelo-Cuautle E., Pano-Azucena A. D., Guillén-Fernández O., Silva-Juárez A. Analog/digital implementation of fractional order chaotic circuits and applications. Berlin/Heidelberg, Germany: Springer.

27. Rossler O. An equation for hyperchaos. Physics Letters A, 1979, 71(2-3), 155–157. https://doi.org/10.1016/0375-9601(79)90150-6

28. Anishchenko V. S., Birukova N. I., Astakhov S. V., Boev Y. I. Poincaré recurrences time and local dimension of chaotic attractors. Rus. J. Nonlin. Dyn, 2012, 8(3), 449–460.

29. Sprott J. C. A proposed standard for the publication of new chaotic systems. International Journal of Bifurcation and Chaos, 2011, 21(09), 2391–2394. https://doi.org/10.1142/S021812741103009X

30. Varan M, Akgul A. Control and synchronisation of a novel seven-dimensional hyperchaotic system with active control. Pramana, 2018, 90(4), 1–8. https://doi.org/10.1007/s12043-018-1546-9

31. Yu W., Wang J., Wang J., Zhu H., Li M., Li Y., et al. Design of a New Seven-Dimensional Hyperchaotic Circuit and Its Application in Secure Communication. IEEE Access, 2019, 7, 125586–125608. https://doi.org/10.1109/ACCESS.2019.2935751

32. Yang Q., Zhu D., Yang L A new 7D hyperchaotic system with five positive Lyapunov exponents coined. International Journal of Bifurcation and Chaos, 2018, 28(5), 1850057. https://doi.org/10.1142/S0218127418500578

33. Hu Z., Chan C. K. A 7-D hyperchaotic system-based encryption scheme for secure fast-OFDM-PON. Journal of Lightwave Technology, 2018, 36(16), 3373–3381. https://doi.org/10.1109/JLT.2018.2841042

34. Sambas A., Vaidyanathan S., Bonny T., Zhang S., Hidayat Y., Gundara G., et al. Mathematical model and FPGA realization of a multi-stable chaotic dynamical system with a closed butterfly-like curve of equilibrium points. Applied Sciences, 2021, 11(2), 788. https://doi.org/10.3390/app11020788

35. Vaidyanathan S., Abba O. A., Betchewe G., Alidou M. A new three-dimensional chaotic system: its adaptive control and circuit design. International Journal of Automation and Control, 2019, 13(1), 101–121. https://doi.org/10.1504/IJAAC.2019.096420

36. Vaidyanathan S, Tlelo-Cuautle E, Sambas A, Grasso F Dynamical Analysis, Synchronization and Circuit Implementation of a New Hyperchaotic System with Line Equilibrium. In 2019 42nd International Convention on Information and Communication Technology, Electronics and Microelectronics. 2019; 153–156. https://doi.org/10.23919/MIPRO.2019.8757210

37. Benkouider K., Bouden T., Halimi M. Dynamical analysis, synchronization and circuit implementation of a new hyperchaotic system with line equilibrium. In 2019 6th international conference on control, decision and information technologies, April; 1717–1722.